



Intracellular Storage Reduces Stoichiometric Imbalances in Soil Microbial Biomass – A Theoretical Exploration

Stefano Manzoni^{1,2*}, Yang Ding³, Charles Warren⁴, Callum C. Banfield³, Michaela A. Dippold^{3,5} and Kyle Mason-Jones⁶

¹ Department of Physical Geography, Stockholm University, Stockholm, Sweden, ² Bolin Centre for Climate Research, Stockholm University, Stockholm, Sweden, ³ Department of Biogeochemistry of Agroecosystems, University of Goettingen, Goettingen, Germany, ⁴ School of Life and Environmental Sciences, University of Sydney, Sydney, NSW, Australia, ⁵ Geo-Biosphere Interactions, University of Tuebingen, Tuebingen, Germany, ⁶ Department of Terrestrial Ecology, Netherlands Institute of Ecology (NIOO-KNAW), Wageningen, Netherlands

OPEN ACCESS

Edited by:

Martin Thullner,
Helmholtz Centre for Environmental
Research (UFZ), Germany

Reviewed by:

Thomas Wutzler,
Max Planck Institute
for Biogeochemistry, Germany
James Andrew Bradley,
Queen Mary University of London,
United Kingdom

*Correspondence:

Stefano Manzoni
stefano.manzoni@natgeo.su.se

Specialty section:

This article was submitted to
Models in Ecology and Evolution,
a section of the journal
Frontiers in Ecology and Evolution

Received: 24 May 2021

Accepted: 09 September 2021

Published: 30 September 2021

Citation:

Manzoni S, Ding Y, Warren C,
Banfield CC, Dippold MA and
Mason-Jones K (2021) Intracellular
Storage Reduces Stoichiometric
Imbalances in Soil Microbial
Biomass – A Theoretical Exploration.
Front. Ecol. Evol. 9:714134.
doi: 10.3389/fevo.2021.714134

Microbial intracellular storage is key to defining microbial resource use strategies and could contribute to carbon (C) and nutrient cycling. However, little attention has been devoted to the role of intracellular storage in soil processes, in particular from a theoretical perspective. Here we fill this gap by integrating intracellular storage dynamics into a microbially explicit soil C and nutrient cycling model. Two ecologically relevant modes of storage are considered: reserve storage, in which elements are routed to a storage compartment in proportion to their uptake rate, and surplus storage, in which elements in excess of microbial stoichiometric requirements are stored and limiting elements are remobilized from storage to fuel growth and microbial maintenance. Our aim is to explore with this model how these different storage modes affect the retention of C and nutrients in active microbial biomass under idealized conditions mimicking a substrate pulse experiment. As a case study, we describe C and phosphorus (P) dynamics using literature data to estimate model parameters. Both storage modes enhance the retention of elements in microbial biomass, but the surplus storage mode is more effective to selectively store or remobilize C and nutrients according to microbial needs. Enhancement of microbial growth by both storage modes is largest when the substrate C:nutrient ratio is high (causing nutrient limitation after substrate addition) and the amount of added substrate is large. Moreover, storage increases biomass nutrient retention and growth more effectively when resources are supplied in a few large pulses compared to several smaller pulses (mimicking a nearly constant supply), which suggests storage to be particularly relevant in highly dynamic soil microhabitats. Overall, our results indicate that storage dynamics are most important under conditions of strong stoichiometric imbalance and may be of high ecological relevance in soil environments experiencing large variations in C and nutrient supply.

Keywords: reserve storage, surplus accumulation, ecological stoichiometry, nutrient limitation, microbial model

INTRODUCTION

Microbial use of soil resources and decomposition of plant residues regulate ecosystem function and even global element cycles (Paul, 2007; Schimel and Schaeffer, 2012). Understanding the modulators of microbial resource use is therefore important. Among these modulators, the ability to internally store resources is a trait that affects both the survival of an individual organism and its overall resource use patterns (Kadouri et al., 2005; Mason-Jones et al., in press). Diverse microorganisms are known to internally store carbon (C), nitrogen (N) or phosphorus (P) (Albi and Serrano, 2016; Koller et al., 2017; Watzer and Forchhammer, 2018). Although intracellular storage is likely a widespread trait among soil microorganisms and may crucially modulate soil biogeochemical cycles (Mason-Jones et al., in press), this trait is yet to be understood in the context of soil microbial growth and survival, in particular from a theoretical perspective.

Numerous storage compounds have been identified in microorganisms, such as glycogen, poly- β -hydroxybutyrate (PHB), and triacylglycerides (TAG) for C storage (Holme and Palmstierna, 1956; Wilkinson, 1963; Alvarez, 2016), as well as polyphosphate for P (Rao et al., 2009; Albi and Serrano, 2016) and cyanophycin for N (Füser and Steinbüchel, 2007; Watzer and Forchhammer, 2018). Storage compounds can enhance microorganisms' resistance to starvation and maintain their viability (Matin et al., 1979; Ruiz et al., 2001; Busuioc et al., 2009). Storage can be especially advantageous in variable environments, by buffering an organism against variations in external resource supply or environmental conditions (Sekar et al., 2020; Mason-Jones et al., in press). Flows to and from storage can constitute significant proportions of resource budgets, particularly on short time scales (i.e., days to weeks) after microbes experience a pulse of C or nutrients (Obruca et al., 2014; Becker et al., 2018; Mason-Jones et al., 2019). Microbes experience high resource availability, but also more competition and potentially large stoichiometric imbalances during resource pulses in the rhizosphere (high C:nutrient ratio) or near decaying plant residues or manure (low C:nutrient ratios in the latter). All these conditions require strategies to rapidly capture resources and sequester them away from competitors. Hence, under these conditions, microbial storage could be quantitatively significant for microbial resource budgets and ultimately for long-term soil organic matter dynamics. However, the role of storage is likely to vary depending on the time scale of storage synthesis and remobilization and microbial growth, in relation to the time scale of resource variations.

Storage traits can be classified into two modes using terminology adapted from plant science (Chapin et al., 1990; Mason-Jones et al., in press): surplus storage and reserve storage. (In the following we treat these strategies as mutually exclusive for simplicity, but they might co-occur.) These modes are defined based on the degree of reliance on resource surplus. Surplus storage occurs when resource availability exceeds immediate requirements for growth or maintenance, so such storage does not compete with other needs (Chapin et al., 1990). For example, when N is limited but C is in excess, diverse microorganisms accumulate PHB, TAG or glycogen (Doi et al., 1992; Ratledge and

Wynn, 2002; Rúa et al., 2008; Wilson et al., 2010; Preiss, 2014; Alvarez, 2016). The advantage of this mode is that it retains the excess resources that otherwise would be lost. In contrast, reserve storage competes for resources with other metabolic demands such as growth and defense (Chapin et al., 1990). This mode can still be advantageous when limiting resources need to be stored for later use—e.g., when resources are stored before a period of severe starvation or unsuitable environmental conditions. These two storage modes—surplus and reserve storage—have been identified in microorganisms (Mason-Jones et al., in press), but their functional significance for stoichiometric relations in soil has not been assessed so far.

Storage of a particular element allows an organism to incorporate resources in stoichiometric proportions very different from the stoichiometry of their 'active' (non-storage) biomass, which can have important effects on ecological interactions from population to ecosystem scales (Sterner and Elser, 2002; Turner et al., 2017). Storing carbon or nutrients in defined compounds can be advantageous when degrading substrates characterized by different elemental composition compared to the active biomass. In plant litter, N and P contents are respectively 10–50 and 100–300 times lower than in biomass, resulting in nutrient limitation; in contrast, soil organic matter and certain amendments such as manure tend to be C-limited (Mooshammer et al., 2014). Despite this wide variation in resource stoichiometry, the C:N:P ratio of the soil microbial biomass is believed to be well-constrained (Cleveland and Liptzin, 2007; Schleuss et al., 2019), and surprisingly similar to the Redfield ratio first described in aquatic ecosystems (Redfield, 1958). Yet there is evidence of significant departures from this ratio in aquatic ecosystems, where the principle was first proposed (Geider and La Roche, 2002; Godwin and Cotner, 2015). Any imbalance between nutrient availability and microbial requirements affects the balance of nutrient mineralization and the transformation and possible stabilization of soil organic matter (Manzoni et al., 2010; Schleuss et al., 2019; Coonan et al., 2020). Therefore, intracellular C-, N- or P-rich storage, by altering whole-organism stoichiometry, allows resource incorporation at seemingly unbalanced element ratios, with implications for these soil functions.

Our understanding of soil functions has been supported by soil biogeochemical modelling, along with integration of microbially explicit models into broader ecosystem and Earth system models (Todd-Brown et al., 2012; Wieder et al., 2018). Current soil C and nutrient cycling models describe the flow of elements through various organic matter compartments and microbial biomass (for a review, see Manzoni and Porporato, 2009). Soil microbes are typically considered a single compartment, without distinction between biomass components involved in metabolic activity and storage components. In most of these models, microbial C:N (and often C:P) ratios are held constant (Manzoni and Porporato, 2009), while in some models, microbial C to nutrient ratios can vary in response to stoichiometric imbalances (Allison, 2012; Fatichi et al., 2019; Manzoni et al., 2021). This allows some effects of storage to be captured at the whole cell or microbial community level, but without explicitly modelling storage dynamics. On the other hand, detailed models that

distinguish among different cellular components do so by setting fixed proportions for each component, possibly depending on microbial functional type (Kaiser et al., 2014). Lacking dynamic regulation of storage, these models cannot describe storage changes in response to variations in element availability. Some models account for specific intracellular compounds in a dynamic way—e.g., osmolytes for cell turgor regulation (Manzoni et al., 2014)—but neglect storage compounds. Mathematically, storage compounds can be treated as additional compartments with their own dynamics, as done in microbial models developed for biotechnology applications (Karahan et al., 2006; Ni et al., 2009) and to describe growth of microbial isolates (Nev and van den Berg, 2017), but this approach has not been used to predict soil C and nutrient cycling so far (with the exception of the C-only model by Tang and Riley, 2015). The consequences of storage of different elements for model predictions thus remain open to question, which frames the scope of this contribution.

To this aim, we implemented the reserve and surplus storage modes into a C and nutrient cycling model suitable to describe short-term incubations of soil samples. Using this model, we address the following questions:

Q1: what are the effects of C storage on C and nutrient allocation by soil microbes along gradients of nutrient availability?

Q2: does combined C and nutrient storage result in qualitatively changed element allocation relative to C storage only?

Q3: to what degree are the two storage modes able to retain C and nutrients in the soil after addition of substrates differing in amount and stoichiometry?

Our results—obtained from model simulations under idealized conditions—should be seen as exploratory analyses of the possible microbial responses to substrate quality and quantity manipulation when intracellular storage is accounted for. As such, these results represent a set of model-generated hypotheses that could be tested in future empirical studies.

THEORY

Mass Balance Equations

Storage compartments (subscript *ST*) are added to a microbial dynamics model with active (non-storage) microbial biomass (subscript *B*) feeding on an externally provided organic substrate (subscript *S*) and—if required—also on inorganic nutrients (subscript *I*). Since the aim of the study is to examine short-term responses of microbial biomass to changes in resource availability (time scales in the order of days to a few weeks), we neglect slower dynamics such as those of native organic matter (time scales in the order of years or longer). Moreover, we assume environmental conditions (soil moisture and temperature) are kept stable to mimic laboratory incubations. The model scheme is shown in **Figure 1**; all symbols are listed and defined in **Table 1**. The mass balances for C and a generic nutrient E (nitrogen or phosphorus) are reported in **Table 2** [Equations (1)–(7)].

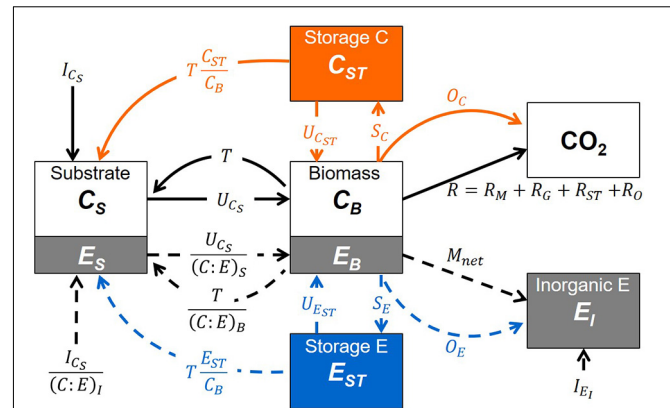


FIGURE 1 | Schematic of the model compartments (boxes) and rates (arrows). Both carbon (C) and a generic nutrient (E, where E = nitrogen or phosphorus) are described as they are transferred from the substrate compartment (subscript S) to the active microbial biomass (B), the storage compounds (ST), and the mineralized products: inorganic nutrient (subscript I) and carbon dioxide (CO₂). C and nutrient flows are depicted by solid and dashed arrows, respectively, while flows to or from storage are shown in orange (carbon) and blue (nutrient); all symbols are defined in **Table 1**. An alternative scenario in which the external nutrient only occurs in inorganic form is presented in **Supplementary Figure 1**.

The active microbial biomass takes up organic C from the substrate at a rate U_{C_S} (first order kinetics with rate constant k_S , suitable for uptake of labile compounds at less than saturating levels), converts it into biomass with a growth efficiency e , and synthesizes storage compounds at a rate S_C . Stored C is remobilized at a rate $U_{C_{ST}}$. To avoid excessive values of C storage that might occur with the surplus storage mode, a fraction of S_C is released when stored C nears the threshold γ_C (expressed as g stored C per g active biomass C). Part of the C taken up is respired at a rate R , including contributions from growth on substrate (R_G), growth on storage (R_{ST}), maintenance (R_M), and overflow respiration (R_O). The R_O represents C mineralization to release excessive C and is thus calculated based on the stoichiometric imbalance of the active microbial biomass (Schimel and Weintraub, 2003). The R_O can also be interpreted as excretion of excess C (e.g., extracellular polysaccharides) or additional C costs associated with nutrient limitation (e.g., synthesis of extracellular enzymes), but for simplicity, in this work we adopt the common mathematical definition of R_O as an overflow mechanism leading to carbon dioxide release. Necromass is produced at a rate T , modelled according to first order kinetics (i.e., $T = mC_B$), and recycled to the substrate pool.

Nutrient flows follow C flows according to the C:E ratios of the compartments where the flows originate. The only exceptions are the rates of E storage synthesis and remobilization (S_E and $U_{E_{ST}}$, respectively) and net E mineralization, which are modelled as pure element flows without any associated C. This is strictly appropriate for P storage as polyphosphate, and a reasonable approximation for N storage as cyanophycin, which has a C:N ratio of just 1.7 (for simplicity we assume no C in the nutrient storage). As for stored C, excess storage E is mineralized when storage contents are approaching the threshold

TABLE 1 | List of symbols and their units (see also **Figure 1**).

Symbol	Definition	Units
State variables (mass balance equations in Table 2)		
C_B	Active microbial biomass C	mg C g soil ⁻¹
C_S	External substrate C	mg C g soil ⁻¹
C_{ST}	Intracellular storage C	mg C g soil ⁻¹
$(C : E)_S$	External substrate C:E ratio	mg C mg E ⁻¹
E_B	Active microbial biomass E	μg E g soil ⁻¹
E_S	External substrate E	μg E g soil ⁻¹
E_{ST}	Intracellular storage E	μg E g soil ⁻¹
E_I	Inorganic E	μg E g soil ⁻¹
C and E flow rates (calculated as a function of the state variables)		
M_{net}	Net E mineralization rate	μg E g soil ⁻¹ d ⁻¹
O_C	Overflow from C storage (surplus mode only)	mg C g soil ⁻¹ d ⁻¹
O_E	Overflow from E storage (surplus mode only)	μg E g soil ⁻¹ d ⁻¹
R	Total microbial respiration rate ($R_G + R_M + R_{ST} + R_O$)	mg C g soil ⁻¹ d ⁻¹
R_G	Respiration rate for growth on substrate C	mg C g soil ⁻¹ d ⁻¹
R_M	Rate of maintenance respiration	mg C g soil ⁻¹ d ⁻¹
R_{ST}	Respiration rate for growth on storage C	mg C g soil ⁻¹ d ⁻¹
R_O	Rate of overflow respiration	mg C g soil ⁻¹ d ⁻¹
S_C	Rate of C storage synthesis	mg C g soil ⁻¹ d ⁻¹
S_E	Rate of E storage synthesis	μg E g soil ⁻¹ d ⁻¹
T	Microbial turnover rate	mg C g soil ⁻¹ d ⁻¹
U_{C_S}	Substrate C uptake rate	mg C g soil ⁻¹ d ⁻¹
$U_{C_{ST}}$	Storage C remobilization rate	mg C g soil ⁻¹ d ⁻¹
$U_{E_{ST}}$	Storage E remobilization rate	μg E g soil ⁻¹ d ⁻¹
U_G	Rate of C made available for growth ($U_{C_S} - S_C + U_{C_{ST}}$)	mg C g soil ⁻¹ d ⁻¹
Model parameters (time invariant)		
$(C : E)_B$	Active microbial biomass C:E ratio	mg C mg E ⁻¹
$(C : E)_I$	Substrate input C:E ratio	mg C mg E ⁻¹
e	Growth efficiency of the active biomass	mg C mg C ⁻¹
I_{C_S}	Rate of external input to substrate C	mg C g soil ⁻¹ d ⁻¹
I_E	Maximum rate of inorganic E immobilization	μg E g soil ⁻¹ d ⁻¹
I_{E_I}	Rate of external input to inorganic E	μg E g soil ⁻¹ d ⁻¹
k_I	Maximum inorganic E immobilization rate constant	d ⁻¹
k_S	Substrate C uptake rate constant	d ⁻¹
$k_{C_{ST}}$	Storage C remobilization rate constant	d ⁻¹
$k_{E_{ST}}$	Storage E remobilization rate constant	d ⁻¹
k_M	Maintenance respiration rate constant	d ⁻¹
$K_{C_{ST}}$	Half-saturation constant for substrate inhibition of C_{ST} remobilization	mg C g soil ⁻¹
$K_{E_{ST}}$	Half-saturation constant for substrate inhibition of E_{ST} remobilization	μg E g soil ⁻¹
m	Microbial turnover rate constant	d ⁻¹
γ_C	Maximum storage C to active microbial C ratio	mg C mg C ⁻¹
γ_E	Maximum storage E to active microbial E ratio	mg E mg E ⁻¹
σ_C	Fraction of C taken up allocated to C reserve storage	-
σ_E	Fraction of E taken up allocated to E reserve storage	-

The generic nutrient E represents either nitrogen (N) or phosphorus (P).

γ_E (only with surplus storage). Finally, the extracellular inorganic E compartment exchanges E with the active biomass via the net E mineralization rate, M_{net} (see section “Stoichiometric Constraints”). The organic substrate C and E, as well as inorganic E compartments can also receive external inputs (for C, I_{C_S} ; for

nutrient E calculated as the ratio of the C input rate and C:E ratio, $I_{C_S} / (C : E)_I$; for the inorganic nutrient, I_{E_I}).

In the following section, we describe in detail the relationship between C and E exchanges involving the active biomass (section “Stoichiometric Constraints”), which is the basis for modelling

TABLE 2 | Mass balance equations for carbon (C) and a generic nutrient (E).

	Change in C or E	Inputs	Substrate uptake	Storage synthesis	Storage remobilization	Turnover and overflow of storage C and E	Respiration or net nutrient mineralization	Eq.
Substrate C	$\frac{dC_S}{dt} =$	I_{C_S}	$-U_{C_S}$			$+T + \frac{C_{ST}}{C_B} T$		(1)
Substrate E	$\frac{dE_S}{dt} =$	$\frac{I_{C_S}}{(C:E)_T}$	$\frac{-U_{C_S}}{(C:E)_S}$			$+ \frac{1}{(C:E)_B} T + \frac{E_{ST}}{C_B} T$		(2)
Active microbial biomass C	$\frac{dC_B}{dt} =$		U_{C_S}	$-S_C$	$+U_{C_{ST}}$	$-T$	$-R_M - R_G - R_O - R_{ST}$	(3)
Active microbial biomass E	$\frac{dE_B}{dt} =$		$\frac{U_{C_S}}{(C:E)_S}$	$-S_E$	$+U_{E_{ST}}$	$-\frac{T}{(C:E)_B}$	$-M_{net}$	(4)
Storage C	$\frac{dC_{ST}}{dt} =$			$+S_C$	$-U_{C_{ST}}$	$-\frac{C_{ST}}{C_B} T - O_C$		(5)
Storage E	$\frac{dE_{ST}}{dt} =$			$+S_E$	$-U_{E_{ST}}$	$-\frac{E_{ST}}{C_B} T - O_E$		(6)
Inorganic E	$\frac{dE_I}{dt} =$	I_{E_I}				$+O_E$	$+M_{net}$	(7)

The balance equation for each compartment occupies a row and rates are grouped along the columns.

the C and nutrient storage modes (sections “Reserve Storage Mode” and “Surplus Storage Modes”). An alternative scenario in which nutrient E only occurs in inorganic form is presented in **Supplementary Information 1**.

Stoichiometric Constraints

The C and nutrient flow rates can be expressed based on the relative demands of the microbial biomass for C and nutrient. These demands are defined on the assumption that the C:E ratio of the active microbial biomass is time-invariant (homeostatic approximation), while we allow overall stoichiometric flexibility via changes in intracellular C and E storage. The homeostatic assumption translates into a relation between the C and nutrient balances of the microbial biomass; i.e., $\frac{dC_B}{dt} = (C : E)_B \frac{dE_B}{dt}$ (Manzoni and Porporato, 2009), which in turn results in the definition of the net nutrient exchanges between microbial biomass and the inorganic nutrient compartment (Equation (10)). This approach is common to most litter and soil C, N and P cycling models (Parton et al., 1988; Manzoni et al., 2010; Fatichi et al., 2019), and can be modified to accommodate decoupled uptake of organic C and inorganic nutrients (see **Supplementary Information**). Using Equation (3) and (4), the homeostatic assumption translates to a mathematical constraint expressing the balance of C and E in the growing biomass (hereafter denoted as ‘stoichiometric constraint’),

$$U_{C_S} - S_C + U_{C_{ST}} - R_M - R_G - R_O - R_{ST} = (C : E)_B \left[\frac{U_{C_S}}{(C : E)_S} - S_E + U_{E_{ST}} - M_{net} \right]. \quad (8)$$

Depending on which element (C or E) is limiting, and on the mode of storage synthesis and remobilization, Equation (8) allows calculating the rates of overflow respiration, net nutrient mineralization, and synthesis and remobilization of C and E storage. To define these rates, it is convenient to first re-write Equation (8) by linking uptake and growth respiration rates via the growth efficiency e . We thus assume that respiration from growth on external substrate is a fixed fraction $1-e$ of the

C uptake that is available for growth after subtracting storage synthesis, $R_G = (1 - e) (U_{C_S} - S_C)$; respiration associated with growth using storage is also a fixed fraction of the rate of growth on storage, $R_{ST} = (1 - e) U_{C_{ST}}$. With these assumptions, and further defining the rate at which C becomes available for growth as $U_G = U_{C_S} - S_C + U_{C_{ST}}$, Equation (8) simplifies to,

$$eU_G - R_M - R_O = (C : E)_B \left[\frac{U_{C_S}}{(C : E)_S} - S_E + U_{E_{ST}} - M_{net} \right]. \quad (9)$$

Under conditions of C limitation, $R_O = 0$, so that Equation (9) provides a definition for the net nutrient mineralization rate as,

$$M_{net} = \frac{U_{C_S}}{(C : E)_S} - S_E + U_{E_{ST}} - \frac{eU_G - R_M}{(C : E)_B}. \quad (10)$$

The net nutrient mineralization rate is positive as long as the supply of the nutrient to the active biomass from other pools (i.e., $U_{C_S} / (C : E)_S + U_{E_{ST}}$) is larger than the demand for the nutrient storage synthesis (S_E) and for growth. The nutrient demand is in turn calculated as the net growth rate (growth after subtracting maintenance costs) divided by microbial C:E ratio [the last term on the right-hand side of Equation (10)]. When E supply is lower than the demand, the net E mineralization rate turns negative, as microbes start immobilizing E from the inorganic E compartment. This condition corresponds to ‘organic nutrient limitation’ (as defined by Wutzler et al., 2017). Under conditions of ‘inorganic nutrient limitation’, M_{net} is bounded by the maximum immobilization rate I_E (i.e., $M_{net} = -I_E$). This represents the maximum amount of inorganic nutrient that can be immobilized per unit time, due to factors that constrain the rate of inorganic nutrient uptake, such as low nutrient availability or limited rate of transport towards the microbial biomass. For simplicity, I_E is modelled by first order kinetics as $I_E = k_I E_I$. If the supply rate of inorganic nutrient is insufficient to meet the demand, conditions shift from being C limited to being E limited, resulting in excess C that is released through overflow respiration (as in Schimel and Weintraub, 2003;

Wutzler et al., 2017). Accordingly, the rate of overflow respiration is obtained from Equation (9) as,

$$R_O = -(C : E)_B \left[\frac{U_{C_S}}{(C : E)_S} - S_E + U_{E_{ST}} + I_E \right] + eU_G - R_M. \quad (11)$$

We can now define a set of ‘rules’ that characterize different modes of storage synthesis and remobilization (Table 3). These modes allow defining S_C , S_E , $U_{C_{ST}}$, and $U_{E_{ST}}$, and thus the rates of net nutrient mineralization and C overflow (Equation (10) and (11), respectively). As a final step, we define mathematically the two storage modes: reserve storage (storage compounds are synthesized whenever the stored element is available) and surplus storage (storage compounds are synthesized whenever the stored element is in excess of stoichiometric demand).

Reserve Storage Mode

In the reserve storage mode, a fixed fraction of the resources taken up is diverted from growth or maintenance to storage. As in previous models applied to biological wastewater treatment systems, C and E storage synthesis rates are defined as fractions σ_C and σ_E of the substrate C and E taken up (Karahan et al., 2006; Ni et al., 2009), after removing C requirements for maintenance,

$$S_C = \max [0, \sigma_C (U_{C_S} - R_M)], \quad (12)$$

$$S_E = \sigma_E \frac{U_{C_S}}{(C : E)_S}. \quad (13)$$

These fractions of uptake are stored irrespective of the stoichiometric balance of the organism, so that some storage takes place even when that resource is limiting, in accordance with the reserve storage concept. In Equation (12), the lower bound at zero is imposed to ensure that the storage synthesis rate does not become negative when substrate C availability is low.

Storage remobilization rates $U_{C_{ST}}$ and $U_{E_{ST}}$ are assumed to decrease when external substrates are abundant, and also depend on storage contents, with the latter modelled for simplicity as a linear dependence (Tang and Riley, 2015), instead of using Monod kinetics as in other models (Karahan et al., 2006; Ni et al., 2009),

$$U_{C_{ST}} = \frac{k_{C_{ST}} C_{ST}}{1 + \frac{C_S}{K_{C_S}}}, \quad (14)$$

$$U_{E_{ST}} = \frac{k_{E_{ST}} E_{ST}}{1 + \frac{E_S}{K_{E_S}}}, \quad (15)$$

where $k_{C_{ST}}$ and $k_{E_{ST}}$ are the rate constants for storage remobilization and K_{C_S} and K_{E_S} are the half-saturation constants for the substrate inhibition effects (e.g., when $C_S = K_{C_S}$, the C storage remobilization rate is reduced to half of the maximum $k_{C_{ST}} C_{ST}$); if K_{C_S} and $K_{E_S} \rightarrow \infty$, substrate inhibition is absent.

Depending on which element is stored (C or E), we can define three specific reserve storage scenarios (Table 3):

- 1) Reserve C (no E storage): $\sigma_C > 0$, $k_{C_{ST}} > 0$, $\sigma_E = 0$
- 2) Reserve E (no C storage): $\sigma_C = 0$, $\sigma_E > 0$, $k_{E_{ST}} > 0$
- 3) Reserve C and E: $\sigma_C > 0$, $k_{C_{ST}} > 0$, $\sigma_E > 0$, $k_{E_{ST}} > 0$

With Equations (12)-(15) defining the rates of storage synthesis and remobilization, and parameters σ_C , σ_E , $k_{C_{ST}}$, and $k_{E_{ST}}$ determining how specific modes are expressed, net nutrient mineralization and overflow respiration rates can accordingly be calculated with Equations (10) and (11) to guarantee a fixed C:E ratio of the active microbial biomass.

Using these definitions of C and E flows to and from storage [Equations (12)-(15)], simultaneous synthesis and remobilization of storage compounds occurs. This ‘futile’ cycle should not be interpreted as a physiological process, but rather as a mathematical description of the controlling factors of storage dynamics leading to a net exchange rate between active biomass and storage.

Surplus Storage Modes

In the surplus storage mode, storage compounds are synthesized only when substrates are in excess of their stoichiometric demand. As a result, depending on which element is stored (C or E), we can define three specific surplus storage scenarios (Table 3):

- 1) Surplus C storage under nutrient-limited conditions (i.e., no overflow respiration) and remobilization under C-limited conditions (no E storage).
- 2) Surplus E storage under C-limited conditions (i.e., no nutrient mineralization) and remobilization under nutrient-limited conditions (no C storage).
- 3) Surplus C storage under nutrient-limited conditions (i.e., no overflow respiration) and surplus E storage under C-limited conditions (i.e., no nutrient mineralization); C and E are remobilized at rates proportional to the amounts of storage C and E, respectively.

In contrast to the reserve storage mode where scenarios were defined by simply changing the values of the storage synthesis and remobilization parameters, here different equations are needed for each scenario because the calculations of excess C and/or E are in each case different. To derive these equations, we further assume that storage C and E can accumulate without limits (i.e., $\gamma_C \rightarrow \infty$ and $\gamma_E \rightarrow \infty$ in the equations in Table 2). This assumption allows for a more intuitive mathematical treatment in sections “Surplus Storage of C (Without E Storage),” “Surplus Storage of E (Without C Storage),” “Surplus Storage of Both C and E,” but is not realistic. Therefore, in the actual model implementation, upper bounds for feasible storage C and E accumulation are also imposed, as described in section “Limit Cases in Surplus Storage Scenarios” (i.e., γ_C and γ_E take finite values in the model used for all analyses). Moreover, in this formulation, stored C is not mobilized to grow on excess available inorganic nutrients. Inorganic nutrients are

TABLE 3 | Summary of the equations describing the rates of overflow respiration (R_O), net nutrient mineralization (M_{net}), storage C synthesis (S_C) and remobilization (U_{CST}), and storage E synthesis (S_E) and remobilization (U_{EST}), for different storage modes (reserve vs. surplus storage), different scenarios for storage elements (C vs. E), and different growing conditions (C vs. E limitation).

Modes of intracellular storage use	Scenarios for stored elements	C or E limitation	R_O	M_{net}	S_C	U_{CST}	S_E	U_{EST}
No storage	None	C	0	(10)	0	0	0	0
		E	(11)	$-I_E$	0	0	0	0
	C	C	0	(10)	(12)	(14)	0	0
		E	(11)	$-I_E$	(12)	(14)	0	0
Reserve storage	E	C	0	(10)	0	0	(13)	(15)
		E	(11)	$-I_E$	0	0	(13)	(15)
	C & E	C	0	(10)	(12)	(14)	(13)	(15)
		E	(11)	$-I_E$	(12)	(14)	(13)	(15)
	C	C	0	0	0	(17)	0	0
		E	0	$-I_E$	(16)	0	0	0
Surplus storage	E	C	0	0	0	0	(18)	0
		E	0	$-I_E$	0	0	0	(19)
	C & E	C	0	0	0	(14)	(20)	(15)
		E	0	$-I_E$	(21)	(14)	0	(15)

Color codes are the same used in Figures 2–5.

only used when the organic substrate is nutrient poor (see the **Supplementary Information Section 1** for an alternative model structure where microbes use organic C and inorganic E).

Surplus Storage of C (Without E Storage)

Under nutrient limitation ($M_{net} = -I_E$), C in excess is stored (so that $R_O = 0$) and no growth on storage occurs ($U_{CST} = 0$). Following these assumptions, Equation (9) yields,

$$S_C = - \left[\frac{1}{e} \frac{(C : E)_B}{(C : E)_S} - 1 \right] U_{C_S} - \frac{R_M}{e} - \frac{(C : E)_B}{e} I_E. \quad (16)$$

Under C limitation, C from storage is used to convert the excess E from the substrate into biomass, while no C storage is synthesized. If all excess E is converted to biomass, $M_{net} = 0$, and recalling that $R_O = 0$, from Equation (9) we find,

$$U_{CST} = \left[\frac{1}{e} \frac{(C : E)_B}{(C : E)_S} - 1 \right] U_{C_S} + \frac{R_M}{e}. \quad (17)$$

When E in the substrate is not in excess and E immobilization is sufficient to meet the stoichiometric demand, storage C is neither synthesized nor remobilized.

Surplus Storage of E (Without C Storage)

Nutrient E is stored when in excess (under C limitation) and used when it is in short supply in the substrate (E limitation). Following the same rationale as in section “Surplus Storage of C (Without E Storage),” but now with a focus on E, using Equation (9) with $R_O = 0$, $M_{net} = 0$ because all excess E is stored, and $U_{EST} = 0$ because no storage remobilization occurs under C limitation, we find,

$$S_E = \left[\frac{1}{(C : E)_S} - \frac{e}{(C : E)_B} \right] U_{C_S} + \frac{R_M}{(C : E)_B}. \quad (18)$$

As in the surplus storage of C, when E in the substrate is not in excess and E immobilization is sufficient to meet the stoichiometric demand, storage E is neither synthesized nor remobilized. Under E limitation, growth on stored E occurs to use excess C for growth and avoid releasing it through overflow respiration, while no storage E is synthesized. Therefore, imposing $R_O = 0$, $M_{net} = -I_E$, and $S_E = 0$ in Equation (9) we find,

$$U_{EST} = - \left[\frac{1}{(C : E)_S} - \frac{e}{(C : E)_B} \right] U_{C_S} - \frac{R_M}{(C : E)_B} - I_E. \quad (19)$$

Surplus Storage of Both C and E

Here both elements can be stored when they are available in the substrate in excess of stoichiometric demands. This allows keeping $R_O = 0$ and $M_{net} = 0$, unless E immobilization becomes necessary after depletion of storage E. Accordingly, under C limitation $M_{net} = 0$ and $S_C = 0$, so that Equation (9) yields,

$$S_E = \left[\frac{1}{(C : E)_S} - \frac{e}{(C : E)_B} \right] U_{C_S} + \frac{R_M - eU_{CST}}{(C : E)_B} + U_{EST}. \quad (20)$$

Under nutrient limitation, imposing $M_{net} = -I_E$, $R_O = 0$, and $S_E = 0$ in Equation (9) yields,

$$S_C = - \left[\frac{1}{e} \frac{(C : E)_B}{(C : E)_S} - 1 \right] U_{C_S} + U_{CST} - \frac{R_M}{e} - \frac{(C : E)_B}{e} (U_{EST} + I_E). \quad (21)$$

Both stored elements are assumed to be remobilized as for the reserve storage mode [Equation (14) and (15)] because surplus storage of either C or E already compensates stoichiometric imbalances, and no additional stoichiometric constraints can be used to define remobilization rates. In other words, from

Equation (9) we can only obtain S_E or S_C (under C or nutrient limitation, respectively), leaving the two remobilization rates mathematically undetermined. As a consequence, remobilization rates must be modelled independently of the stoichiometric constraints for all the flow rates to be mathematically specified.

Limit Cases in Surplus Storage Scenarios

All the surplus storage scenarios could allow unrealistic levels of storage accumulation, because storage synthesis is defined according to stoichiometric constraints—not physiological limits to storage. To avoid reaching excessive storage accumulation, C and E stores are capped by defining maximum ratios of storage to active biomass, respectively denoted as γ_C and γ_E . As the maximum storage values are approached, overflow mechanisms are mathematically defined to divert C or E to either CO₂ or inorganic E, and are denoted as ‘excess storage synthesis’ rates. These rates are defined as fractions $C_{ST}/(\gamma_C C_B)$ or $E_{ST}/(\gamma_E E_B)$ of the storage synthesis rates for storage E or C, respectively (Table 2),

$$O_C = \frac{C_{ST}}{\gamma_C C_B} S_C, \quad (22)$$

$$O_E = \frac{E_{ST}}{\gamma_E E_B} S_E. \quad (23)$$

In the extreme case of $C_{ST}/C_B = \gamma_C$ or $E_{ST}/E_B = \gamma_E$, excess storage synthesis equals S_C or S_E and thus surplus C or E from the organic substrate is not routed to storage, but immediately removed from the active microbial biomass. In the reserve storage mode, the storage C and E contents are dynamically capped by the remobilization rates, so no excess storage synthesis is implemented.

Moreover, the amount of available storage might not be sufficient to compensate for limited substrate C or E availability in the surplus storage scenarios. For example, a large input of nutrient poor substrate might require more than the available stored E to convert excess C in the substrate into biomass. To prevent rapid storage remobilization from driving the storage compartment into negative values, the storage remobilization rate is constrained so that at most it reaches the values set by Equation (14) and (15). In these limit cases when the threshold values of remobilization are reached, stored compounds can only partially compensate stoichiometric imbalances and excess E and C are respectively released via net E mineralization and overflow respiration.

Initial Conditions and Model Parameters

The model formulation is general, but in the numerical analyses we consider the case of P as a limiting nutrient. Accordingly, the modeled storage P compartment consists of polyphosphate, a widespread microbial P storage compound (Rao et al., 2009). The model is parameterized to describe C and P contents and flow rates in a soil sample amended with a large amount of organic C and a variable amount of organic P. Our aim is to explore the system behavior rather than calibrate and validate the

model for a specific dataset, which would not be feasible with the current published data on microbial internal storage. Therefore, parameters were estimated from the literature if possible, or varied in sensitivity analyses when values were particularly uncertain (Table 4).

Initial conditions for the numerical simulations and model parameters were chosen to represent a short-term laboratory incubation experiment where environmental conditions such as temperature and soil moisture are kept stable (Table 4). The initial intracellular storage of both C or E is set to 5% of the corresponding element in the active biomass. This low value captures the conditions of non-growing microbial biomass, and helps avoid a large initial rate of storage remobilization, which—combined with high initial substrate uptake—would make interpretation difficult. The C:P ratio of the initial substrate as well as the amount of initial substrate are both allowed to vary to explore responses to resource stoichiometry and addition rates (Figure 2).

Kinetic parameters are chosen to capture reasonable time scales of the modelled processes: the rate constants for substrate uptake (k_S), maximum inorganic E immobilization (k_I), and storage remobilization ($k_{C_{ST}}$ and $k_{E_{ST}}$) are assumed to be 1 d⁻¹ (corresponding to a turnover time of 1 day), the rate constants of microbial turnover (m) and maintenance respiration (k_M) are assumed to be 0.05 d⁻¹ (turnover time of 20 days). The microbial growth efficiency is set to $e = 0.5$, a reasonable value for a labile substrate with a degree of reduction comparable to that of biomass (Roels, 1980). The C:P ratio of the active microbial biomass is assumed to be 20 g C g P⁻¹—a value within the range observed for temperate grasslands or deciduous forests (Xu et al., 2013).

For simplicity, we assumed that storage can be accumulated to at most 50% of the same element in the active biomass (i.e., $\gamma_C = \gamma_P = 0.5$). These values are conservatively set lower than maximum storage fractions reported for C (Koller et al., 2017) and P (Anand and Aoyagi, 2019). In the reserve storage mode, 20% of the C and P taken up are assumed to be stored ($\sigma_C = \sigma_P = 0.2$). This value is lower than the >50% efficiency of conversion of substrate C to storage C that has been observed under C surplus (Obruca et al., 2014), but likely more representative of soil conditions. Finally, we assume that storage remobilization is reduced by half when the external substrate C and P contents are equal to half the biomass C and P contents, respectively (i.e., $K_{C_{ST}}$ and $K_{E_{ST}}$ equal half of the initial biomass C and P contents, respectively).

Given the large uncertainties, a sensitivity analysis to test the effect of varying $k_{C_{ST}}$, $k_{P_{ST}}$, $K_{C_{ST}}$, $K_{E_{ST}}$, σ_C , and σ_P within relatively broad ranges was conducted and is provided in the Supplementary Information Section 2.

Numerical Experiments

A schematic of the three numerical experiments is shown in Figure 2. First, the C and P flow rates are calculated for the different storage modes and growing conditions of Table 3, as a function of substrate C:P ratio, for fixed compartment sizes; i.e., C and nutrient contents are set to their baseline values from Table 4 (Figure 2A). This scenario represents a static snapshot

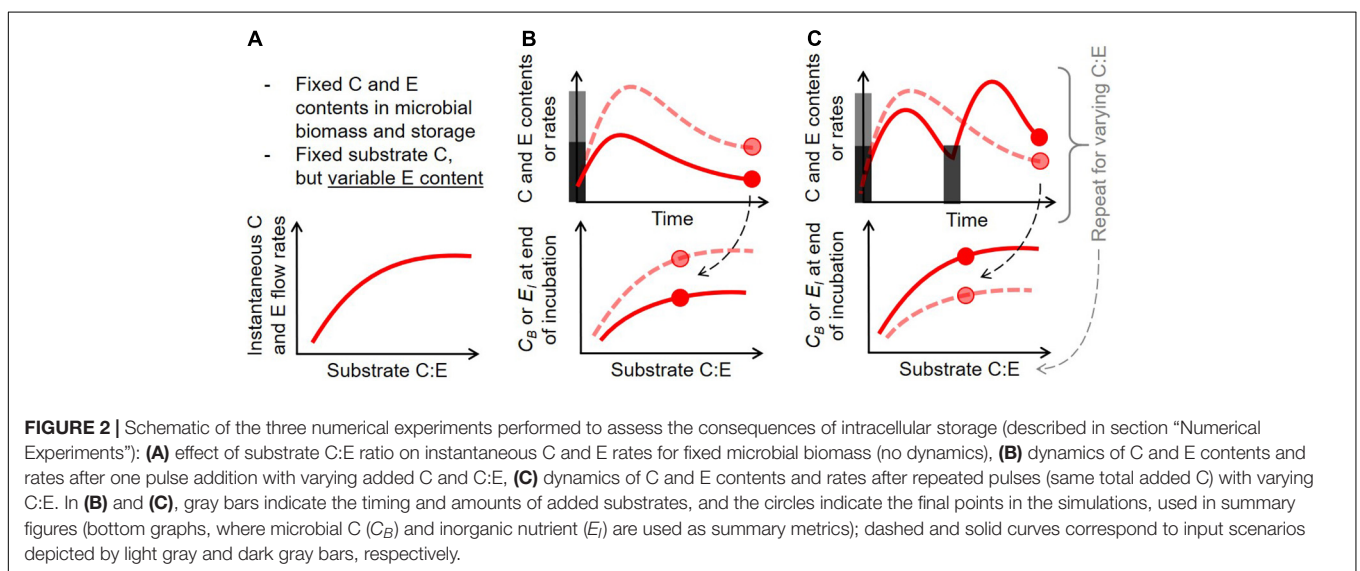
TABLE 4 | Initial conditions and parameter values.

Symbol	Value or relation to other parameters	Units	Explanation or data source
Initial conditions (also used as baseline values)			
$C_B(0)$	1	mg C g soil ⁻¹	Chosen value
$C_S(0)$	0.5 to 2	mg C g soil ⁻¹	2 in Figures 3-7 ; 0.5 to 2 in Figures 8, 9
$C_{ST}(0)$	= 0.05 $C_B(0)$	mg C g soil ⁻¹	5% of initial microbial C
$(C:P)_S(0)$	1 to 200	mg C mg E ⁻¹	Varied in sensitivity analyses
$P_B(0)^1$	= 10 ³ $C_B(0)/(C:P)_B$	μg P g soil ⁻¹	Value based on microbial C:P ratio
$P_S(0)^1$	= 10 ³ $C_S(0)/(C:P)_S(0)$	μg P g soil ⁻¹	Value based on initial substrate C:P ratio
$P_{ST}(0)$	= 0.05 $P_B(0)$	μg P g soil ⁻¹	5% of initial microbial P
$P_i(0)$	1 to 100	μg P g soil ⁻¹	Varied in sensitivity analyses
Model parameters			
$(C:P)_B$	20	mg C mg P ⁻¹	Xu et al. (2013)
e	0.5	mg C mg C ⁻¹	Roels (1980)
l_{C_S}	0 (variable in Figure 9)	mg C g soil ⁻¹ d ⁻¹	Assumption of closed system (except in the numerical experiment with repeated substrate additions)
l_{P_i}	0	μg P g soil ⁻¹ d ⁻¹	Assumption of closed system
k_l	1	d ⁻¹	Equal rate constants for C and P uptake and remobilization
k_S	1	d ⁻¹	Equal rate constants for C and P uptake and remobilization
$k_{C_{ST}}^2$	1	d ⁻¹	Equal rate constants for C and P uptake and remobilization
$k_{P_{ST}}^2$	1	d ⁻¹	Equal rate constants for C and P uptake and remobilization
k_M	0.05	d ⁻¹	Assumed
$K_{C_{ST}}^2$	= 0.5 $C_B(0)$	mg C g soil ⁻¹	Assumed relation to initial biomass C
$K_{P_{ST}}^2$	= 0.5 $E_B(0)$	μg P g soil ⁻¹	Assumed relation to initial biomass P
m	0.05	d ⁻¹	Assumed
γ_C	0.5	mg C mg C ⁻¹	Consistent with observations (Koller et al., 2017)
γ_P	0.5	mg P mg P ⁻¹	Consistent with observations (Anand and Aoyagi, 2019)
σ_C^2	0.2	-	Consistent with observations (Obruca et al., 2014)
σ_P^2	= σ_C	-	Assumed relation to σ_C

The initial conditions are used both as starting points in the dynamic simulations and as baseline values when showing instantaneous C and P flow rates.

¹ Numerical values in front of the symbolic expression includes unit conversion from mg to μg.

² Parameters varied in a sensitivity analysis (**Supplementary Information Section 2**).



of the variations in C and P flow rates that would happen when only the P content in the substrate changes, and neglects the dynamics of the system (the mass balance equations are not solved through time). All combinations of storage modes and the storage element scenarios are compared, using a model version in which no storage is implemented as reference.

Second, the dynamics are studied by simulating through time idealized laboratory conditions in which a given amount of substrate is added to a soil sample with specified initial conditions (initial active biomass, storage and extracellular inorganic nutrient contents; **Figure 2B**). All the storage element scenarios are compared, again using a model version without storage as reference. To illustrate the outcomes of different storage modes along the whole numerical experiment, the active biomass C and extracellular inorganic P contents at the end of the simulations are calculated, and shown as a function of initial substrate amount and C:P ratio.

Third, the dynamics are studied under repeated substrate additions (**Figure 2C**). To allow a comparison across simulations, the total added C is fixed to the same amount as in the single addition experiment, but the number of additions is varied between 2 and 32. Final active biomass C and extracellular inorganic P contents are shown as a function of the number of substrate additions and the C:P ratio of the added substrate.

RESULTS

Carbon and Nutrient Flow Rates When Varying Substrate C:P Ratio

In **Figures 3, 4**, changes in C and P flow rates are shown as a function of substrate C:P ratio, here increased by letting substrate P vary at constant substrate C content, so that the rate of C uptake remains fixed.

Reserve Storage

When reserve storage is used (**Figure 3**), the accumulation and remobilization of stored C and P do not fully compensate stoichiometric imbalances. As a result, overflow respiration increases (**Figure 3A**) and net P mineralization decreases (**Figure 3D**) with increasing substrate C:P to maintain stable active biomass C:P. The net P mineralization becomes negative first (at C:P between 40 and 50 g C g P⁻¹), and then reaches the maximum immobilization rate at a C:P ranging between 50 and 70 g C g P⁻¹, depending on the specific reserve storage scenario. At this point, overflow respiration starts increasing as microbes become P limited at high C:P. However, at a given substrate C:P, overflow respiration is lower and net P mineralization higher when microbes store C or C and P than in microbes without intracellular storage. This is due to C being diverted from growth to storage, which decreases P demand and thus increases P mineralization relative to microbes without storage. In contrast, microbes storing only P exhibit comparable overflow respiration, but lower net P mineralization than microbes without storage.

Increasing the C:P ratio does not affect storage C synthesis and remobilization (**Figures 3B,C**) because, with the reserve storage mode, storage C synthesis depends only on the rate of substrate

C uptake [Equation (12)] and the storage remobilization rate depends on the amount of substrate C and stored C (here fixed), not on the substrate C:P ratio [Equations (14)]. These rates are nevertheless shown for completeness to allow comparisons with the corresponding panels in **Figure 4**. In contrast, the rate of P reserve synthesis decreases with increasing substrate C:P because of decreasing organic P uptake rate [**Figure 3E**; Equation (13)], whereas the rate of storage P remobilization increases because at high substrate C:P, storage P remobilization is less inhibited [**Figure 3F**; Equation (15)].

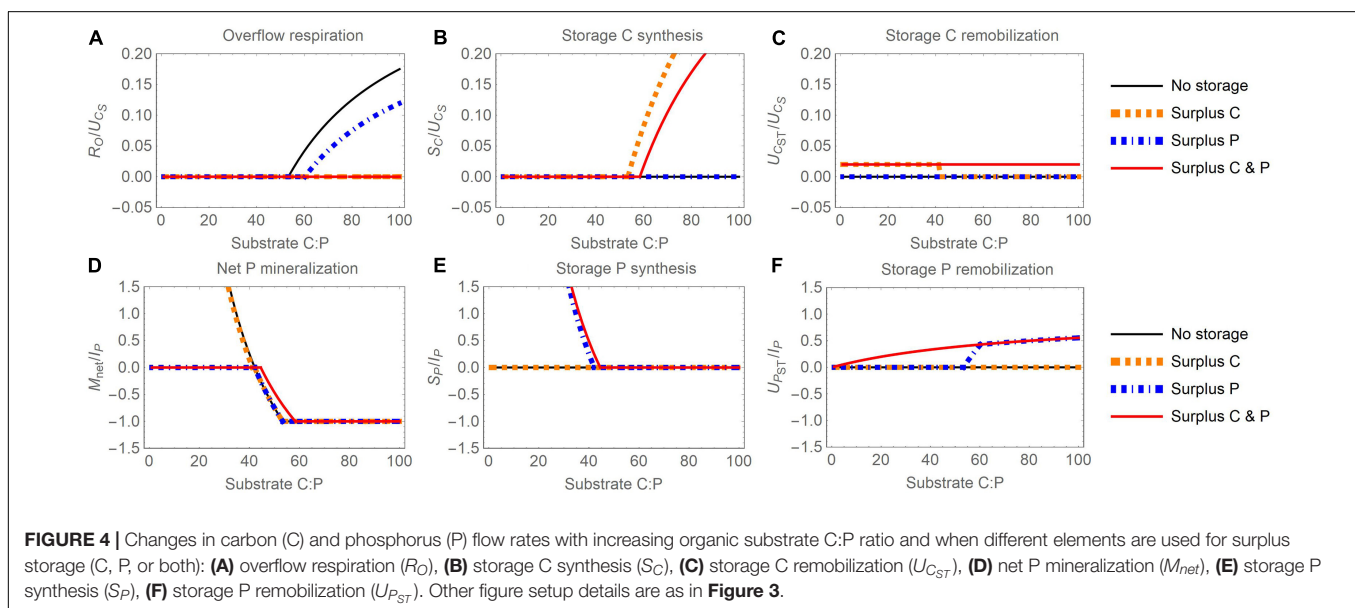
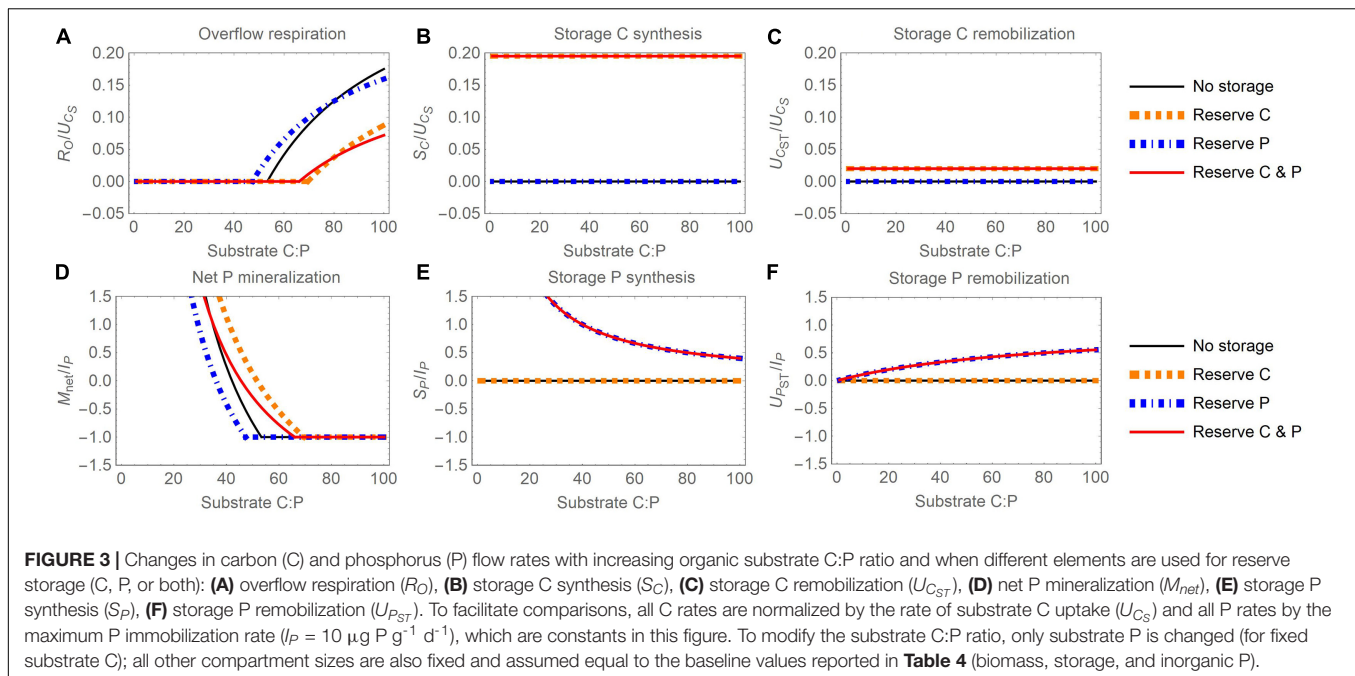
Surplus Storage

Thanks to the compensation of stoichiometric imbalances, overflow respiration is lower with surplus storage than with reserve storage, or even zero throughout the C:P range shown (compare **Figures 3A, 4A**). Under C-limited conditions, the net P mineralization rate is maintained at zero for the surplus P and C and P scenarios (**Figure 4D**). Under P-limited conditions, the net P mineralization rates in the surplus C and surplus P modes are equivalent to P mineralization without storage. In contrast, in the surplus C and P scenario, mineralization is shifted towards higher C:P ratios, similar to the reserve storage case, because storage remobilization in this scenario is defined in the same way for both modes (compare the red curves in **Figures 3D, 4D**).

Different from reserve storage, the rates of C storage accumulation and remobilization in the three scenarios of surplus storage vary with substrate stoichiometry. Surplus C accumulates in storage at high substrate C:P (**Figure 4B**) and surplus P accumulates at low C:P (**Figure 4E**). Storage C and P are remobilized at low and high C:P ratios, respectively, in the surplus scenarios storing exclusively C or P (**Figures 4C,F**), whereas both C and P are remobilized in the C and P surplus storage scenario. This is because remobilization in the C and P surplus storage scenario is proportional to the stored C and P contents [Equations (14)-(15)]. At low C:P, storage C remobilization in the surplus C and surplus C and P scenarios are equal (**Figure 4C**) because the amount of C remobilization required to fulfil stoichiometric demand is very high at high substrate P availability. Under these conditions, the remobilization rate in the surplus C scenario becomes limited by the amount of stored C (Section 2.4.4), exactly as assumed in the C and P scenario [Equations (14)-(15)]. The same mechanism explains the equal P remobilization rates in the surplus P and surplus C and P scenarios at high C:P (**Figure 4F**).

Temporal Changes in Carbon and Phosphorus Compartments and Flow Rates

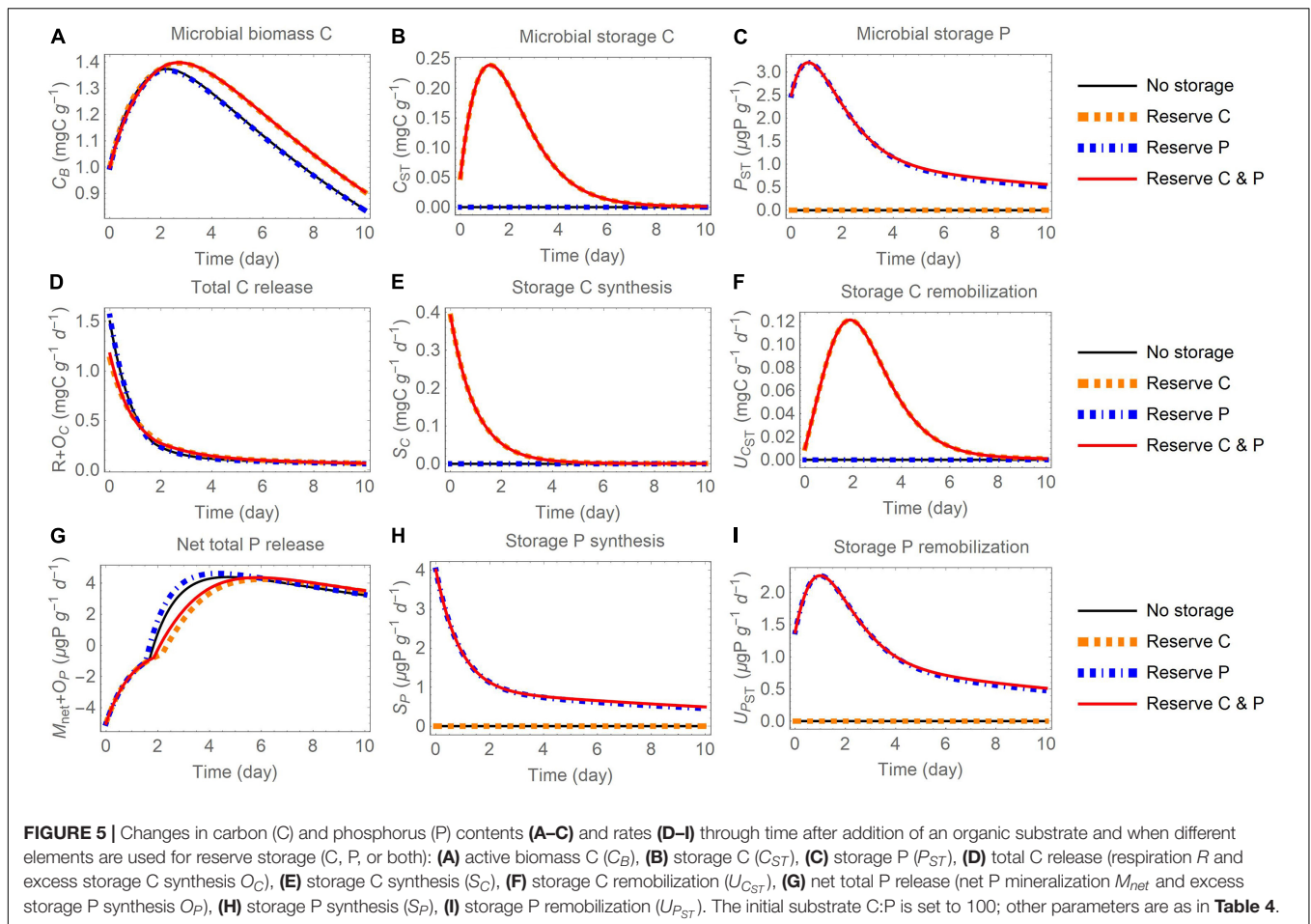
Having presented a snapshot of soil C and nutrient flow rates in section “Carbon and Nutrient Flow Rates When Varying Substrate C:P Ratio,” we now run the model through time, starting from the initial conditions reported in **Table 4** (initial substrate C:P = 100 g C g P⁻¹), and compare results obtained by assuming different storage modes and scenarios. **Figures 5, 6** show results for the reserve and surplus storage



modes, respectively, and **Figure 7** shows a comparison between the two modes when both elements can be used as storage.

In all model runs the initial substrate is depleted within the week-long simulation. Because the uptake rate is modelled as linear (dependent only on substrate amount), in all simulations the dynamics of substrate consumption are comparable (small variations are induced by microbial turnover feeding into the substrate compartment) and this similarity allows for a comparison across storage modes and scenarios. In general, microbial biomass increases during the initial phase, reaches a peak, and then decreases as mortality and maintenance respiration become larger than growth when substrate is

depleted (panels A in **Figures 5–7**). The rate of C release from the active biomass (respiration and excess storage C synthesis) follows a decreasing trend, mostly due to the reduction in growth respiration as the substrate is depleted (**Figures 5D, 6D, 7B**). Conversely, the rate of P release (net P mineralization and excess storage P synthesis) increases from negative values (net P immobilization) in the initial phase, when the P-poor substrate does not provide sufficient P for microbial growth and conditions are P limited, to progressively higher values, eventually turning into net P release when the substrate has been enriched in organic P from microbial turnover and conditions have become C limited



(Figures 5G, 6G, 7C). These general trends are qualitatively consistent across storage modes and scenarios, but the specific dynamics of microbial growth, respiration, and P mineralization differ due to the contrasting patterns of C and P storage accumulation and remobilization.

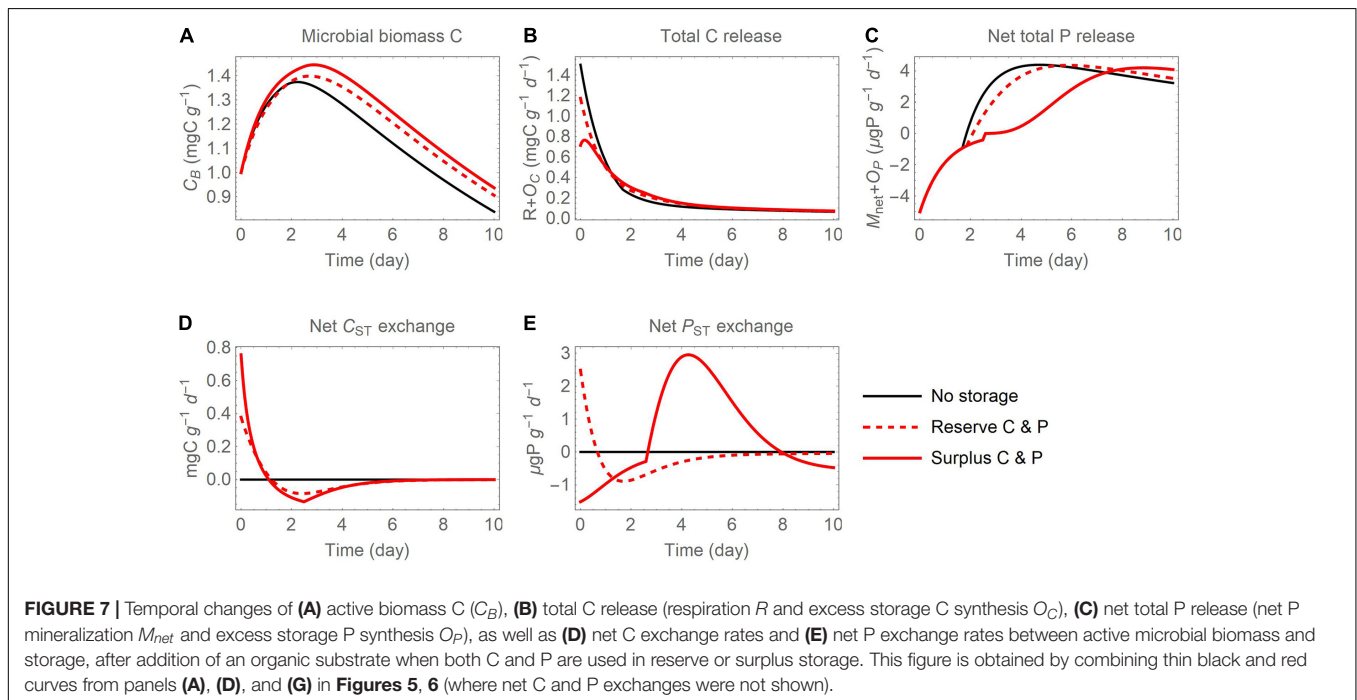
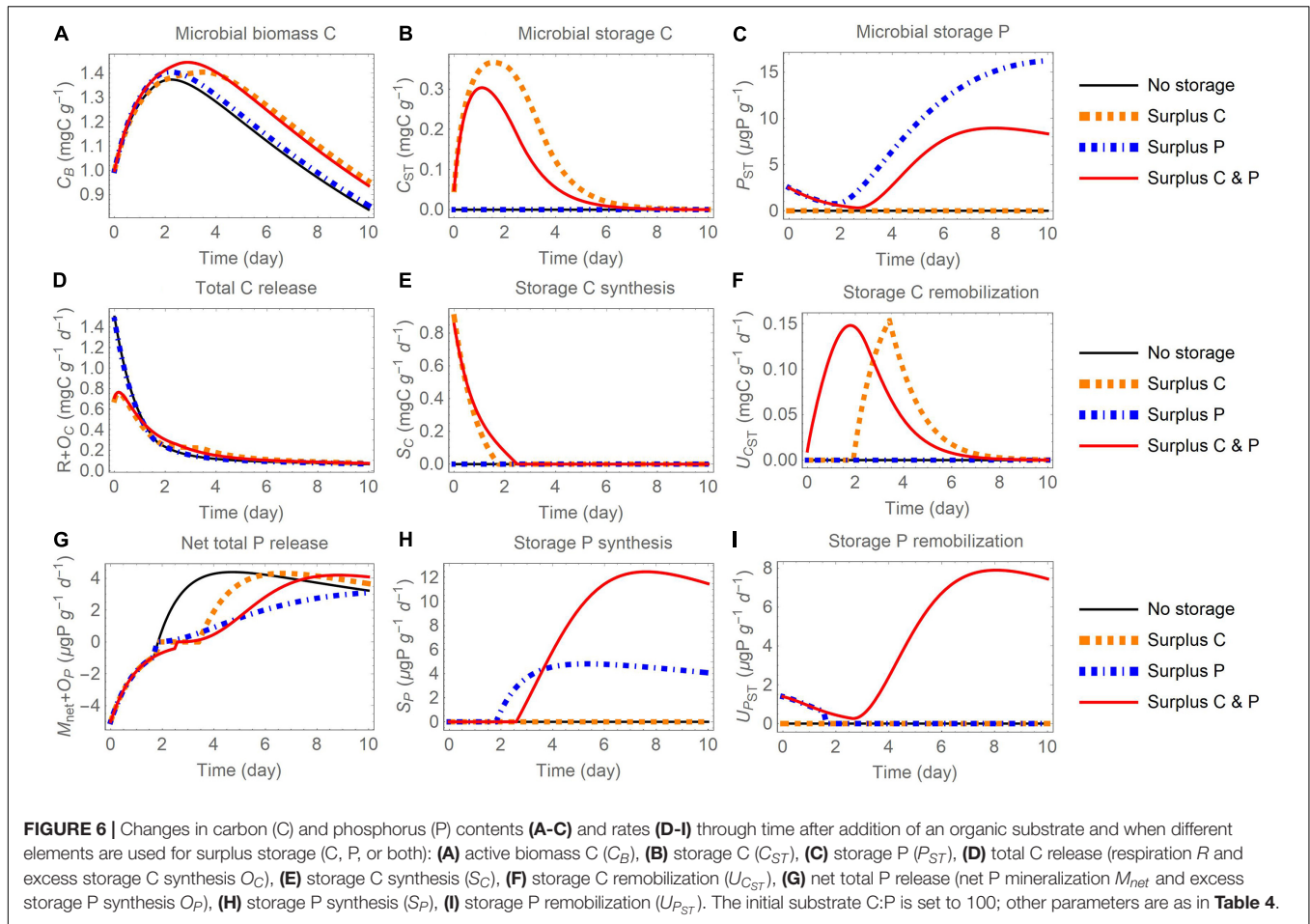
Reserve Storage

When the reserve storage mode is adopted, the contents of stored C and/or P increase early during the incubation, when rates of organic C and P uptake are high, and decrease later as the substrate is depleted (Figures 5B,C). These patterns in storage contents are due to initially high rates of storage synthesis (Figures 5E,H), followed after approximately two days by a peak in the rates of storage remobilization (Figures 5F,I). Compared to scenarios where only P is stored, or no storage is used, storing C (or C and P) helps buffering variations in substrate C, providing an advantage in terms of microbial growth (Figure 5A), made possible by lower respiration (Figure 5D; recall that with reserve storage $O_C = 0$), and reduced net P mineralization rate (Figure 5G; recall that $O_P = 0$). The effect of storage P appears minor relative to the scenario without storage (comparable dot-dashed blue and thin black curves in Figure 5), because in this particular simulation the substrate contains little P and the initial P storage is small. Therefore, storing P alone

does not have a large impact on microbial growth with these initial conditions.

Surplus Storage

When the surplus storage mode is adopted, the content of stored C increases early during the incubation, because C is in excess and is transferred to the storage compartment (Figures 6B,E). In contrast, P storage increases late in the incubation, when C has been consumed and P is in excess (Figures 6C,H). Also, stored C is remobilized only when P is in excess (dotted orange curve in Figure 6F), while stored P is remobilized when C is in excess and the microbes are P limited in the initial phase of the incubation (dot-dashed blue curve in Figure 6I). The remobilization of both storage C and storage P occurs continuously in the C and P surplus storage scenario, because remobilization rates are defined as a function of external and stored C and P contents, as explained in section “Surplus Storage of Both C and P” (red curves in Figures 6F,I). Similar to the reserve storage mode, storing C (or C and P) increases microbial growth and decreases respiration (Figures 6A,D). Storing only P is not beneficial in terms of biomass growth, but allows P to be retained in storage rather than to be released to the environment, as indicated by the lower net P mineralization rate in the late phase of the incubation compared to the other scenarios (dot-dashed blue curve in Figure 6G).



In this mode, excess storage synthesis is activated when the storage compartments become large relative to the active biomass. The contribution of excess storage C synthesis remains small compared to respiration (**Supplementary Figures 5A,B**). In contrast, the contribution of excess storage P synthesis to microbial P release is large late in the simulation (**Supplementary Figures 5C,D**), when P is abundant and, due to slow growth rates, not all available P can be used for growth nor can it be stored. As a result, while by definition $M_{net} = 0$ under C limitation, a delayed P release via excess storage synthesis occurs.

Comparison Between Storage Modes

A direct comparison of microbial biomass C, total respiration, and net P mineralization between the reserve and surplus storage modes (C and P scenario) is presented in **Figure 7**. The surplus storage mode (solid red curves) allows microbes to grow more compared to the reserve storage mode (dashed red curves), thanks to lower respiration losses and higher P retention. Not using storage (thin black curves) is comparatively less advantageous, as the initial stoichiometric imbalance in the substrate is not compensated and excess resources are released to the environment—C is released first through high overflow respiration, and P later via P mineralization.

As a summary of the dynamics of storage C and P, the net rates of C and P exchanges between active biomass and storage are compared in **Figures 7D,E**. In both storage modes, storage C accumulates early in the simulation and is depleted later, as conditions move from P limited to C limited. The accumulation and depletion of storage P instead differ between modes. In the reserve mode, storage P is accumulated first and is then depleted, whereas in the storage mode the pattern is reversed and a peak in P accumulation occurs around day 4–5.

Storage Effects Under Varying Substrate C:P Ratio and C Amount

The simulations shown in section “Temporal Changes in Carbon and Phosphorus Compartments and Flow Rates” are obtained for a single initial substrate content with a specified C:P ratio. Here we extend our analyses to explore how a range of substrate contents and a range of initial C:P ratios affect active microbial biomass growth and P mineralization (**Figure 8**). We conducted simulations for all the usual scenarios (shown in **Supplementary Figures 6–9**), but focus here on storage of only C (**Figures 8A,C**) or both C and P (**Figures 8B,D**). To isolate the effect of storage compounds, **Figure 8** shows relative changes between the end points of simulations where microbes use intracellular storage, and reference simulations without storage.

Both reserve and surplus storage modes promote microbial growth compared to the reference simulations (positive values in **Figures 8A,B**). This effect is particularly strong under conditions of marked P limitation; i.e., at high initial substrate contents (darker shades) and high initial C:P ratios. At high initial substrate C:P, storing only C promotes growth in the surplus storage mode slightly more than storing both C and P, since this storage scenario is the most effective at reducing C losses under strong P limitation (compare solid curves in **Figures 8A,B**). In contrast, storing only C in the reserve storage mode is not as

advantageous as storing both C and P at high initial substrate C:P ratios, when reserve storage is unable to reduce overflow C losses (compare dashed curves in **Figures 8A,B**). Moreover, the microbial growth enhancement is stronger when using surplus storage compared to reserve storage at high substrate C:P (solid vs. dashed curves in **Figure 8**).

Surplus storage of only C as well as of both C and P strongly decreases P mineralization, as shown by negative changes in inorganic P at the end of the simulations (solid curves in **Figures 8C,D**). This effect is expected because storage is modelled to compensate stoichiometric imbalances, which should reduce P release. Reserve storage of C has a weak negative effect on inorganic P and reserve storage of C and P has a small positive effect, especially at low initial C supply and initial C:P (dashed curves in **Figures 8C,D**). This positive effect is due to mineralization of the initial intracellular storage P. Both storage modes are more effective at retaining P when the substrate is P-poor, compared to substrate with more balanced C:P.

Storage Effects Under Varying Substrate C:P Ratio and Frequency of Substrate Additions

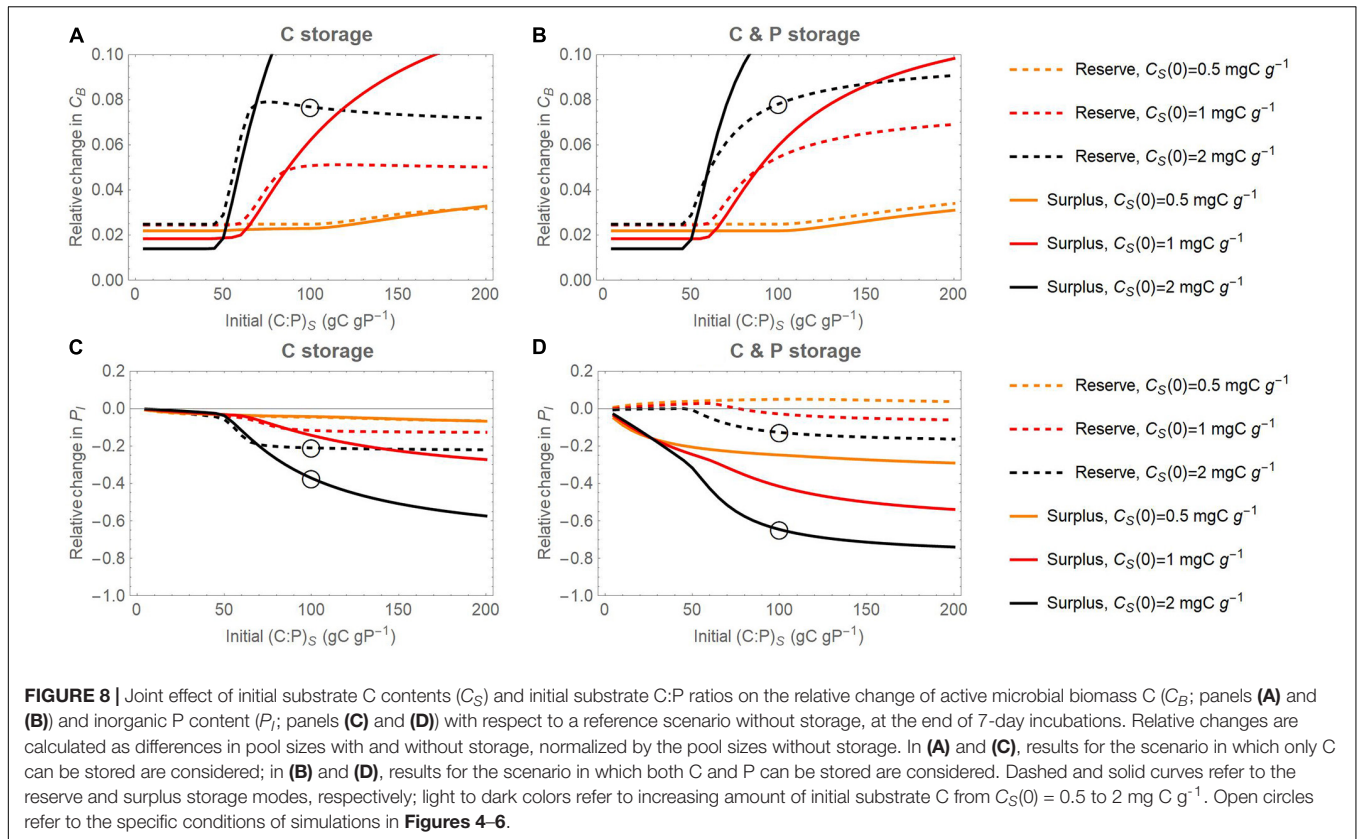
The effect of repeated substrate pulses is assessed as before by comparing active microbial biomass growth and inorganic P, at the end of 21-day simulations (compared to the shorter 7-day simulations of **Figure 8**), in storage scenarios relative to the reference scenario without storage (**Figure 9**). Similar to **Figure 8A**, higher substrate C:P increases the final microbial biomass increments compared to the reference scenario, but this effect depends on the number of substrate additions. For a given C:P ratio, a larger number of additions (with lower amount of C per addition, so that the total added C is fixed) decreases final biomass increments in all storage modes (compare darker and lighter shades in **Figure 9A**). Depending on the number of additions and initial substrate C:P ratio, the final biomass achieved with reserve storage can be higher (generally at low initial C:P) or lower than that achieved with surplus storage (generally at high initial C:P).

At the end of the 21-day simulations, inorganic P is always higher than the value in the reference scenario when microbes adopt reserve storage, for any substrate C:P ratio, whereas the opposite is true for surplus storage. The higher inorganic P is due to mineralization of both initial intracellular P and microbial necromass, whose contribution is higher in these longer simulations compared to the previous numerical experiment. A higher number of substrate additions (darker shades in **Figure 9B**) increases inorganic P at high C:P and lowers inorganic P at low C:P, compared to the single addition experiment.

DISCUSSION

Modelling Approaches for Microbial Intracellular Storage

Ecological implications of internal storage are discussed in sections “What Are the Effects of C Storage on C and Nutrient

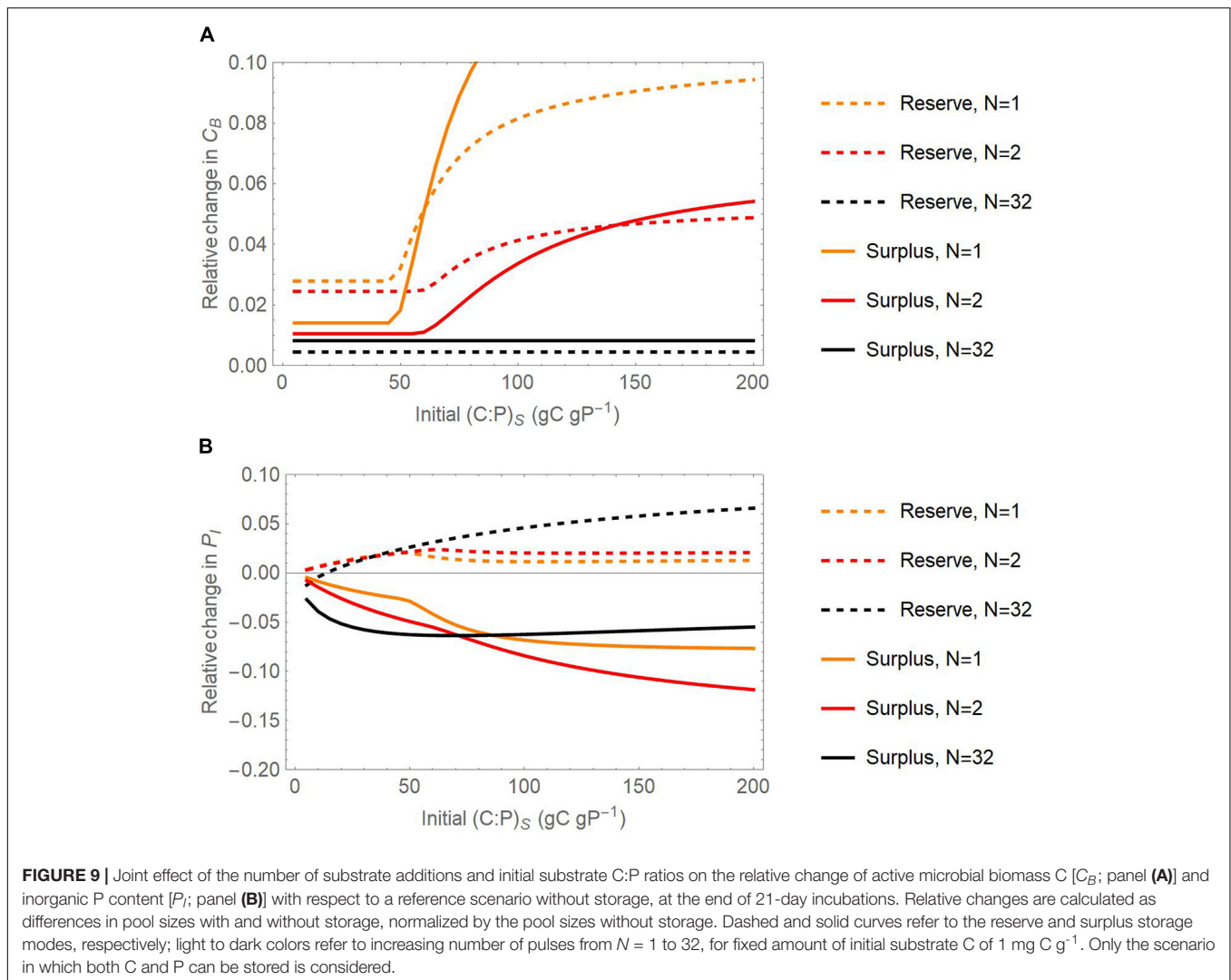


Allocation by Soil Microbes Along Gradients of Nutrient Availability?” and “Does Combined C and Nutrient Storage Result in Qualitatively Changed Element Allocation Relative to C Storage Only?”, but we first consider some technical aspects of modelling storage. The dynamics of intracellular nutrient stores have been previously described in population models for phytoplankton (for a review, see Wang and Hsu, 2019) and bacteria (e.g., Parnas and Cohen, 1976). In phytoplankton models, a ‘cell quota’ is defined as the mass of nutrient per cell, and a mass balance equation for the nutrient is coupled to a population balance equation. In those models, nutrients that are taken up from the growing medium are accumulated in the intracellular storage, which is then used to support cell growth and duplication (Wang and Hsu, 2019). This approach is comparable to our reserve storage mode, except that we allow a fraction of the nutrients taken up to directly support growth [Equations (12) and (13)]. Our approach to reserve storage is thus similar to that implemented in activated sludge models (Karahan et al., 2006; Ni et al., 2009). Other bacterial growth models are based on more complex resource allocation schemes. For example, storage accumulation may be mediated by dynamic assimilation pathways that are up- and down-regulated by both external nutrient availability and storage contents (Nev and van den Berg, 2017).

Storage remobilization is defined in the reserve storage mode as proportional to the amount of existing storage, with an inhibition effect as external resources increase. This formulation

is qualitatively similar to that employed in phytoplankton and activated sludge models, though different kinetics laws have been proposed for this process (Karahan et al., 2006; Ni et al., 2009; Wang and Hsu, 2019). The dynamic energy balance (DEB) models for unicellular organisms assume that resources are assimilated into storage and then remobilized for growth and maintenance at a rate proportional to the amount stored (Tolla et al., 2007; Tang and Riley, 2015). In our model, maintenance costs are instead paid from the resources assimilated rather than from storage (**Figure 1**). In more complex models, stored resources are allocated to a range of cellular functions, including machinery for resource acquisition, maintenance of such machinery, and growth (Nev and van den Berg, 2017). These more complex models are suitable to describe intracellular storage dynamics of microbial isolates, for which detailed data for parameterization might be available. In contrast, we take a simpler approach, in common with most whole-community soil biogeochemical models, where (active) microbial biomass is described by a single ‘well mixed’ compartment. This is necessary to maintain a parsimonious representation in models that might be applied under diverse conditions and at large scales (e.g., Todd-Brown et al., 2012).

Recent growth models for microbial isolates described the accumulation of different nutrients and compounds in storage compartments (Nev and van den Berg, 2017), as we have done here for C and a single macro-nutrient. The main difference



with respect to the model by Nev and van den Berg (2017) is that in their case stoichiometric imbalances were reduced by allocating cellular resources to acquisition of the least available nutrients, while in our case, nutrient uptake *per se* is not regulated and the dynamics of storage provide the required buffering capacity. Despite these differences, the qualitative results are comparable, suggesting that multiple resource use modes can alleviate stoichiometric imbalances (Manzoni et al., 2021).

What Are the Effects of C Storage on C and Nutrient Allocation by Soil Microbes Along Gradients of Nutrient Availability?

Our model results show that storage of C alone enables higher C allocation to active biomass, whether by way of reserve or surplus storage. On the one hand, biomass size is particularly enhanced by storage at high substrate C:P ratios, due to the rerouting of C from overflow respiration to storage, which later supports growth when C limitation returns. This stoichiometric buffering is stronger for surplus storage than for reserve storage. On the other

hand, at low C:P ratios the remobilization of pre-existing stored C provides a supplementary C source, allowing higher biomass growth on the excess of available P. As a consequence of the C mass balance, higher biomass C corresponds to lower cumulative respiration, and therefore carbon use efficiency (defined as active biomass increment over C uptake) is also increased by storage, at least in the relatively short incubations we modelled. Higher biomass and more efficient utilization of C and nutrients indicate an advantage of storage for microorganisms, since these resources are not lost but instead used for growth. Microbial biomass is considered to be the first step toward carbon stabilization in soil organic matter (Cotrufo et al., 2013; Liang et al., 2017), suggesting that storage of C may also help to retain C in the soil system over longer periods of time if the additional biomass C is eventually stabilized in the soil (see also section “To What Degree Are the Two Storage Modes Able to Retain C and Nutrients in the Soil After Addition of Substrates Differing in Amount and Stoichiometry?”). It is notable that this effect would not depend on the direct stabilization of C storage compounds, most of which are remobilized and exhausted over the duration of our

simulation. Rather, stoichiometric buffering by storage leads to enhanced efficiency of (non-storage) biomass growth.

We assumed that excess C is mineralized through overflow mechanisms, which may result in overestimation of the positive effects of C storage on biomass growth. Other processes that we have not considered here could reduce stoichiometric imbalances without resulting in C loss, such as flexible allocation to C *vs.* nutrient acquiring extracellular enzymes (Mooshammer et al., 2014; Wutzler et al., 2017), resulting in degradation of nutrient-rich organic matter when C-rich labile substrates are available (also referred to as nutrient mining, Craine et al., 2007). It is also possible that nutrient retention is increased compared to C losses during senescence under nutrient limitation (Manzoni et al., 2021). Moreover, microbes could excrete excess C instead of storing it internally. If the excreted C is in dissolved form, it could still be lost via leaching, similar—from the cell perspective—to overflow respiration. However, if excreted C accumulates in extracellular polysaccharides, it could play a role in maintaining hydration and possibly supply microbes with C at a later time (Brangari et al., 2018). These alternative nutrient use modes could avoid C mineralization (and potential loss), even without intracellular storage, thus complementing intracellular storage to buffer stoichiometric imbalances.

Storage of C, without P storage, consistently reduces P mineralization. This is a by-product of the larger active biomass, which retains more nutrients. Microbial C storage therefore enhances not only carbon use efficiency but also nutrient use efficiency, suggesting a role for C storage in modulating nutrient mineralization in soils. Reduced mineralization may be viewed as desirable or detrimental, depending on whether mineralization promotes beneficial plant growth or nutrient loss. In our simplified model setup, nutrients not retained in biomass are regarded as lost from the perspective of microbial biomass, but in real soils these nutrients can have various fates. They can be taken up by plants or stabilized on mineral surfaces, thus becoming unavailable to microbes, but they could also remain in the soil solution, from which they could be immobilized by microbes at a later time if the organic nutrient supply decreases. Therefore, the fate of nutrients will depend, in part, on how the dynamics of microbial storage are coupled to carbon supply and nutrient demand in the broader ecosystem. Placing microbial storage in its biogeochemical and ecological context presents research challenges for the future.

Based on our results, it might appear that both forms of intracellular storage are winning strategies compared to lack of storage. However, this is because our model only considers the direct costs of the stored resources. There may be attendant costs for synthesizing storage compounds and developing storage structures, as well as in allocating intracellular space to storage. Motile organisms will also incur energy costs from moving storage around (Pond, 1981), and increased predation risk is conceivable (Lima, 1986). These costs and trade-offs have not been experimentally quantified in microorganisms, and therefore were not considered in the model. The relative advantage of intracellular storage for microbial fitness will need to be reassessed when empirical evidence of these tradeoffs becomes available.

Does Combined C and Nutrient Storage Result in Qualitatively Changed Element Allocation Relative to C Storage Only?

The ability to store C and P, rather than C alone, did not qualitatively change the patterns of C allocation to biomass and respiration in our simulations. Storage pools under surplus storage develop differently over time depending on which element is stored, but this must be interpreted with some caution since different rules of storage remobilization were used to overcome the modelling constraints of stoichiometrically uncoupled C and P storage. As a result of our assumptions, all C and P scenarios have a level of continuous remobilization, causing similarities in the remobilization patterns of the two modes.

Surplus storage of C and P temporarily reduces P mineralization more than C storage alone (Figure 6G). This is expected, since excess P is stored instead of mineralized. This effect is less apparent in the case of reserve storage (Figure 5G), partly because nutrients initially stored in the microbial biomass are mineralized, while this contribution is not present in the scenarios without P storage. If we assumed no initial nutrient storage, all storage modes would result in net retention of nutrients compared to the reference scenario (results not shown).

Since including P storage does not strongly change the results obtained with C storage alone, to a first approximation, it might be feasible to model the effects of C storage in soil without explicitly accounting for simultaneous storage of other nutrients. This could be a helpful simplification for future work, not least because supporting data on polyphosphate and cyanophycin contents in soil are still lacking (Mason-Jones et al., in press). This result is partly a consequence of our simulation setup. In all simulations with this setup, after an initial phase, C becomes the limiting element for microbial growth, so that P storage plays a smaller role than C storage for sustaining long-term growth.

It should also be noted that P release by extracellular enzymes could lead to de-coupled C and P acquisition, in contrast to our assumption of microbial uptake of organic compounds containing both C and P. However, even in the alternative case of de-coupled uptake of organic C and inorganic P, we found similar responses of C and P flow rates to changes in resource C:P ratio (Supplementary Section 1), suggesting that storage of C might follow similar dynamics regardless of the source (organic *vs.* inorganic) of these elements, and also regardless of whether P is stored as well.

To What Degree Are the Two Storage Modes Able to Retain C and Nutrients in the Soil After Addition of Substrates Differing in Amount and Stoichiometry?

Surplus storage has generally larger effects on C and P allocation than reserve storage, with the differences most pronounced at high substrate C:P ratios and large substrate amounts. These conditions might resemble those in the rhizosphere, where C-rich compounds are exuded at high concentrations in the

vicinity of a growing root. The effect of storage is particularly strong in short-term incubations (**Figure 8**), when microbial mortality plays a minor role. However, in longer simulations with repeated substrate additions, nutrients are returned to the substrate compartment via mortality and eventually mineralized, leading to smaller reductions in net nutrient release (**Figure 9**). This comparison between numerical experiments illustrates that the consequences of storage vary depending on the time scale considered. In the long term, storage effects on soil C stabilization and nutrient availability depend on how necromass is stabilized (Cotrufo et al., 2013; Liang et al., 2017). If a large part of necromass eventually becomes stable organic matter, the effect of internal storage would be large, because storage promotes C and nutrient retention in biomass. At the other end of the spectrum of possible necromass fates, if all necromass is decomposed, the role of internal storage would be minor, because any C and nutrient accumulation in biomass would be temporary. These long-term processes are neglected here, given the focus of this contribution on short-term responses to resource addition and stoichiometry. However, coupling our storage dynamics model to a complete soil biogeochemical model could offer insights on the fate of internally stored C and nutrients.

Spreading substrate supply over an increasing number of smaller pulses reduces the relative advantage for biomass of surplus storage compared to a single large pulse. The comparison of pulse frequencies provides a gradient from high temporal resource variability (single pulse) to relatively constant resource supply (32 pulses), which indicates that surplus storage could be particularly favorable under highly variable environments (as also shown experimentally by Sekar et al., 2020). A possible consequence is that storage strategies could be selected in environments with high but intermittent resource availability (transient hotspots), such as in the rhizosphere (Kuzaykov and Blagodatskaya, 2015) or along macropores that transport resources only during heavy rainfall events. Copiotrophic organisms could benefit from storage in these environments by exploiting resources when available and even if stoichiometrically imbalanced.

Overall, the simulations suggest that C and P allocations are sensitive to C storage, and in particular the surplus storage mode, whereas P storage has little effect on C allocation. When substrate supply is high, strongly nutrient-poor, and temporally variable (large resource pulses with long starvation periods), the greater stoichiometric buffering of surplus storage provides larger benefits for C and nutrient efficiency than reserve storage (**Figure 9**). In these numerical experiments, however, resource pulses were regarded as deterministic—i.e., occurring at predetermined time intervals. In natural, randomly varying environments, we expect similar benefits to appear as well, and those benefits would increase in environments with more intermittent resource availability. For example, resource variations can be particularly high in the rhizosphere, where exudation rates vary in response to fluctuations in gross productivity (Kuzaykov and Gavrichkova, 2010), or in the bulk soil when resources occasionally become available during drying-rewetting cycles (Manzoni et al., 2020). These natural variations in resource availability are stochastic, as they

depend on random fluctuations in environmental conditions that affect photosynthesis, or random rainfall events, respectively. We have not analysed the advantages of storage in stochastic environments with our model, but evolution of storage traits might be particularly advantageous (i.e., to maximize fitness) under high resource variability and predictability of resource supply (Fischer et al., 2011). Future work could explore the role of stochastic environments with the proposed model.

Implications for Future Experiments

Extraction of intracellular C and nutrient storage compounds from soil microbial biomass remains a challenge, making it difficult to directly test the theoretical predictions presented here. However, results in **Figure 7** suggest a possible approach based on isotopically labelled substrate additions. **Figures 7C,E** show that the timing of nutrient release varies depending on storage mode. Surplus storage causes accumulation of P in the intermediate phase of the incubation, when P is already abundant while growth starts decreasing due to substrate depletion. This in turn reduces P release compared to microbes adopting reserve storage or no storage. Addition of a nutrient poor substrate with labelled P and C could allow tracking P release from substrate decomposition in isolation from mineralization of native organic P. Addition of a nutrient rich substrate would result in contrasting patterns of both C and nutrient release during the incubation (results not shown). While it is conceptually simple to test model predictions using this type of data for individual microbial taxa, the response of a soil community is more complex because it reflects the proportions of the microbial community expressing differing storage modes. Therefore, varying the substrate C:P ratio in combination with labelling of either P or both C and P would offer insights into the storage modes expressed by microbial isolates, but potentially also—though only at an aggregated level—by whole microbial communities.

Furthermore, metabolic flux analysis based on position-specific labelled precursors of storage molecules combined with subsequent fragment-specific isotope analysis of the produced storage compounds is able to disentangle metabolic C fluxes through storage-forming pathways. As previously done for glycolysis and gluconeogenesis (Wu et al., 2020), biosynthetic and catabolic fluxes can be disentangled and thus both storage modes may be quantified in metabolic tracing experiments.

Conclusion

We developed a microbial biomass growth model that differentiates between an active biomass compartment and intracellular storage compartments for C and/or a nutrient. Storage compartments and associated flow rates were modelled according to two storage modes: reserve storage and surplus storage. The model was used in a theoretical exploration of how the two storage modes interact with carbon and nutrient input quantity, quality (stoichiometry), and timing to shape microbial biomass and extracellular inorganic nutrient dynamics. These transformations of C and nutrients may have implications for long-term C stabilization and short-term nutrient budgets in soil. Our theoretical results suggest the following two hypotheses, to be tested in future experiments:

Hypothesis 1: both reserve storage and surplus storage modes enhance short-term retention of C and nutrients in active biomass, thereby potentially promoting long-term accumulation of C and organic nutrients in soil.

Hypothesis 2: microbial taxa that store resources are expected to be more frequent in environments with more variable resource availability and less nutritionally balanced resources. As a consequence, storage (especially surplus storage) is especially selected for among copiotrophic microorganisms.

DATA AVAILABILITY STATEMENT

The original contributions presented in the study are included in the article/**Supplementary Material**, further inquiries can be directed to the corresponding author/s.

AUTHOR CONTRIBUTIONS

SM and KM-J designed the study and developed the theory, with feedback from all other authors. SM implemented the model and produced the results. SM, KM-J, and YD drafted the manuscript. All authors commented and revised the manuscript.

FUNDING

This project has received funding from the European Research Council (ERC) under the European Union's Horizon 2020 Research and Innovation Programme (grant agreement no 101001608). YD is supported by the German Research Foundation (DFG Ba 6982/1-1). CW is supported by the

Australian Research Council (DP200102565). Open access publication fees are funded by Stockholm University.

ACKNOWLEDGMENTS

We thank two reviewers for their constructive criticism.

SUPPLEMENTARY MATERIAL

The Supplementary Material for this article can be found online at: <https://www.frontiersin.org/articles/10.3389/fevo.2021.714134/full#supplementary-material>

Supplementary 1 | Microbial growth on organic carbon and inorganic nutrients. Supplementary theory and results for the scenario in which C and E acquisition are decoupled, and microbes can utilize C only from an organic source and E only from an inorganic one (**Supplementary Figure 1**). Instantaneous C and P flow rates as a function of organic C to inorganic P ratio are shown for the reserve storage (**Supplementary Figure 2**) and the surplus storage modes (**Supplementary Figure 3**).

Supplementary 2 | Sensitivity analysis. Supplementary analysis showing how results are impacted by uncertainties in model parameter values (**Supplementary Figure 4**), including technical details on how the sensitivity analysis was performed.

Supplementary 3 | Supplementary figures. Supplementary figures illustrating: respiration rate, net P mineralization rate, and excess storage synthesis for C and P (**Supplementary Figure 5**); effects of storage mode (reserve or surplus storage) and storage scenario (C only, P only, C and P scenarios) on microbial biomass C (**Supplementary Figures 6, 8**) and inorganic P contents (**Supplementary Figures 7, 9**) at the end of simulated incubations, when varying initial substrate C contents and initial substrate C:P ratio (**Supplementary Figures 6, 7**), or varying number of substrate additions and initial substrate C:P ratio (**Supplementary Figures 8, 9**).

REFERENCES

- Albi, T., and Serrano, A. (2016). Inorganic polyphosphate in the microbial world. Emerging roles for a multifaceted biopolymer. *World J. Microbiol. Biotechnol.* 32:27. doi: 10.1007/s11274-015-1983-2
- Allison, S. D. (2012). A trait-based approach for modelling microbial litter decomposition. *Ecol. Lett.* 15, 1058–1070. doi: 10.1111/j.1461-0248.2012.01807.x
- Alvarez, H. M. (2016). Triacylglycerol and wax ester-accumulating machinery in prokaryotes. *Biochimie* 120, 28–39. doi: 10.1016/j.biochi.2015.08.016
- Anand, A., and Aoyagi, H. (2019). A High throughput isolation method for phosphate-accumulating organisms. *Sci. Rep.* 9:18083. doi: 10.1038/s41598-019-53429-2
- Becker, K. W., Collins, J. R., Durham, B. P., Groussman, R. D., White, A. E., Fredricks, H. F., et al. (2018). Daily changes in phytoplankton lipidomes reveal mechanisms of energy storage in the open ocean. *Nat. Commun.* 9:5179. doi: 10.1038/s41467-018-07346-z
- Brangari, A. C., Fernández-García, D., Sanchez-Vila, X., and Manzoni, S. (2018). Ecological and soil hydraulic implications of microbial responses to stress – A modeling analysis. *Adv. Water Resour.* 116, 178–194. doi: 10.1016/j.advwatres.2017.11.005
- Busuioac, M., Mackiewicz, K., Buttaro, B. A., and Piggot, P. J. (2009). Role of intracellular polysaccharide in persistence of *Streptococcus mutans*. *J. Bacteriol.* 191, 7315–7322. doi: 10.1128/JB.00425-09
- Chapin, F. S., Schulze, E. D., and Mooney, H. A. (1990). The ecology and economics of storage in plants. *Annu. Rev. Ecol. Syst.* 21, 423–447. doi: 10.1146/annurev.es.21.110190.002231
- Cleveland, C. C., and Liptzin, D. (2007). C:N:P stoichiometry in soil: is there a “Redfield ratio” for the microbial biomass? *Biogeochemistry* 85, 235–252. doi: 10.1007/s10533-007-9132-0
- Coonan, E. C., Kirkby, C. A., Kirkegaard, J. A., Amidy, M. R., Strong, C. L., and Richardson, A. E. (2020). Microorganisms and nutrient stoichiometry as mediators of soil organic matter dynamics. *Nutr. Cycl. Agroecosystems* 117, 273–298. doi: 10.1007/s10705-020-10076-8
- Cotrufo, M. F., Wallenstein, M. D., Boot, C. M., Deneff, K., and Paul, E. (2013). The Microbial Efficiency-Matrix Stabilization (MEMS) framework integrates plant litter decomposition with soil organic matter stabilization: do labile plant inputs form stable soil organic matter? *Glob. Change Biol.* 19, 988–995. doi: 10.1111/gcb.12113
- Craine, J. M., Morrow, C., and Fierer, N. (2007). Microbial nitrogen limitation increases decomposition. *Ecology* 88, 2105–2113. doi: 10.1890/06-1847.1
- Doi, Y., Kawaguchi, Y., Koyama, N., Nakamura, S., Hiramitsu, M., Yoshida, Y., et al. (1992). Synthesis and degradation of polyhydroxyalkanoates in *Alcaligenes eutrophus*. *FEMS Microbiol. Lett.* 103, 103–108. doi: 10.1111/j.1574-6968.1992.tb05827.x
- Fatih, S., Manzoni, S., Or, D., and Paschalis, A. (2019). A mechanistic model of microbially mediated soil biogeochemical processes: a reality check. *Glob. Biogeochem. Cycles* 33, 620–648. doi: 10.1029/2018GB006077
- Fischer, B., Dieckmann, U., and Taborsky, B. (2011). When to store energy in a stochastic environment. *Evolution* 65, 1221–1232. doi: 10.1111/j.1558-5646.2010.01198.x
- Füser, G., and Steinbüchel, A. (2007). Analysis of genome sequences for genes of cyanophycin metabolism: identifying putative cyanophycin metabolizing prokaryotes. *Macromol. Biosci.* 7, 278–296. doi: 10.1002/mabi.200600207

- Geider, R. J., and La Roche, J. (2002). Redfield revisited: variability of C:N:P in marine microalgae and its biochemical basis. *Eur. J. Phycol.* 37, 1–17. doi: 10.1017/S0967026201003456
- Godwin, C. M., and Cotner, J. B. (2015). Aquatic heterotrophic bacteria have highly flexible phosphorus content and biomass stoichiometry. *ISME J.* 9, 2324–2327. doi: 10.1038/ismej.2015.34
- Holme, T., and Palmstierna, H. (1956). Changes in glycogen and nitrogen-containing compounds in *Escherichia coli* B during growth in deficient media. I. Nitrogen and carbon starvation. *Chem. Acta Chem. Scand* 10, 578–586. doi: 10.3891/acta.chem.scand.10-0578
- Kadouri, D., Jurkevitch, E., Okon, Y., and Castro-Sowinski, S. (2005). Ecological and agricultural significance of bacterial polyhydroxyalkanoates. *Crit. Rev. Microbiol.* 31, 55–67. doi: 10.1080/10408410590899228
- Kaiser, C., Franklin, O., Dieckmann, U., and Richter, A. (2014). Microbial community dynamics alleviate stoichiometric constraints during litter decay. *Ecol. Lett.* 17, 680–690. doi: 10.1111/ele.12269
- Karahan, O., Van Loosdrecht, M. C. M., and Orhon, D. (2006). Modeling the utilization of starch by activated sludge for simultaneous substrate storage and microbial growth. *Biotechnol. Bioeng.* 94, 43–53. doi: 10.1002/bit.20793
- Koller, M., Maršálek, L., de Sousa Dias, M. M., and Braunnegg, G. (2017). Producing microbial polyhydroxyalkanoate (PHA) biopolyesters in a sustainable manner. *New Biotechnol.* 37, 24–38. doi: 10.1016/j.nbt.2016.05.001
- Kuzuyakov, Y., and Blagodatskaya, E. (2015). Microbial hotspots and hot moments in soil: Concept & review. *Soil Biol. Biochem.* 83, 184–199. doi: 10.1016/j.soilbio.2015.01.025
- Kuzuyakov, Y., and Gavrichkova, O. (2010). REVIEW: time lag between photosynthesis and carbon dioxide efflux from soil: a review of mechanisms and controls. *Glob. Change Biol.* 16, 3386–3406. doi: 10.1111/j.1365-2486.2010.02179.x
- Liang, C., Schimel, J. P., and Jastrow, J. D. (2017). The importance of anabolism in microbial control over soil carbon storage. *Nat. Microbiol.* 2:17105. doi: 10.1038/nmicrobiol.2017.105
- Lima, S. (1986). Predation risk and unpredictable feeding conditions – Determinants of body-mass in birds. *Ecology* 67, 377–385. doi: 10.2307/1938580
- Manzoni, S., Chakrawal, A., Fischer, T., Schimel, J. P., Porporato, A., and Vico, G. (2020). Rainfall intensification increases the contribution of rewetting pulses to soil heterotrophic respiration. *Biogeosciences* 17, 4007–4023. doi: 10.5194/bg-17-4007-2020
- Manzoni, S., Chakrawal, A., Spohn, M., and Lindahl, B. D. (2021). Modeling microbial adaptations to nutrient limitation during litter decomposition. *Front. For. Glob. Change* 4:686945. doi: 10.3389/ffgc.2021.686945
- Manzoni, S., and Porporato, A. (2009). Soil carbon and nitrogen mineralization: theory and models across scales. *Soil Biol. Biochem.* 41, 1355–1379. doi: 10.1016/j.soilbio.2009.02.031
- Manzoni, S., Schaeffer, S. M., Katul, G., Porporato, A., and Schimel, J. P. (2014). A theoretical analysis of microbial eco-physiological and diffusion limitations to carbon cycling in drying soils. *Soil Biol. Biochem.* 73, 69–83. doi: 10.1016/j.soilbio.2014.02.008
- Manzoni, S., Trofymow, J. A., Jackson, R. B., and Porporato, A. (2010). Stoichiometric controls dynamics on carbon, nitrogen, and phosphorus in decomposing litter. *Ecol. Monogr.* 80, 89–106. doi: 10.1890/09-0179.1
- Mason-Jones, K., Banfield, C. C., and Dippold, M. A. (2019). Compound-specific ¹³C stable isotope probing confirms synthesis of polyhydroxybutyrate by soil bacteria. *Rapid Commun. Mass Spectrom.* 33, 795–802. doi: 10.1002/rcm.8407
- Mason-Jones, K., Robinson, S., Veen, G. F., Manzoni, S., and van der Putten, W. H. (in press). Microbial storage and its implications for soil ecology. *ISME J.* doi: 10.1038/s41396-021-01110-w
- Matin, A., Veldhuis, C., Stegeman, V., and Veenhuis, M. (1979). Selective advantage of a *Spirillum* sp. in a carbon-limited environment. Accumulation of poly-β-hydroxybutyric acid and its role in starvation. *J. Gen. Microbiol.* 112, 349–355. doi: 10.1099/00221287-112-2-349
- Mooshammer, M., Wanek, W., Zechmeister-Boltenstern, S., and Richter, A. (2014). Stoichiometric imbalances between terrestrial decomposer communities and their resources: mechanisms and implications of microbial adaptations to their resources. *Front. Microbiol.* 5:22. doi: 10.3389/fmicb.2014.00022
- Nev, O. A., and van den Berg, H. A. (2017). Variable-internal-stores models of microbial growth and metabolism with dynamic allocation of cellular resources. *J. Math. Biol.* 74, 409–445. doi: 10.1007/s00285-016-1030-4
- Ni, B.-J., Fang, F., Rittmann, B. E., and Yu, H.-Q. (2009). Modeling microbial products in activated sludge under feast-famine conditions. *Environ. Sci. Technol.* 43, 2489–2497. doi: 10.1021/es8026693
- Obruca, S., Benesova, P., Oborna, J., and Marova, I. (2014). Application of protease-hydrolyzed whey as a complex nitrogen source to increase poly(3-hydroxybutyrate) production from oils by *Cupriavidus necator*. *Biotechnol. Lett.* 36, 775–781. doi: 10.1007/s10529-013-1407-z
- Parnas, H., and Cohen, D. (1976). Optimal strategy for metabolism of reserve materials in microorganisms. *J. Theor. Biol.* 56, 19–55. doi: 10.1016/S0022-5193(76)80044-6
- Parton, W. J., Stewart, J. W. B., and Cole, C. V. (1988). Dynamics of C, N, P and S in grassland soils - a model. *Biogeochemistry* 5, 109–131. doi: 10.1007/BF02180320
- Paul, E. A. ed (2007). *Soil Microbiology, Ecology and Biochemistry*. New York, NY: Elsevier. doi: 10.1016/B978-0-08-047514-1.50005-6
- Pond, C. (1981). “Storage,” in *Physiological Ecology*, eds C. R. Townsend, and P. Calow (Oxford: Blackwell Scientific), 190–219.
- Preiss, J. (2014). Glycogen: biosynthesis and regulation. *EcoSal Plus* 6, 1–28. doi: 10.1128/ecosalplus.ESP-0015-2014
- Rao, N. N., Gómez-García, M. R., and Kornberg, A. (2009). Inorganic polyphosphate: essential for growth and survival. *Annu. Rev. Biochem.* 78, 605–647. doi: 10.1146/annurev.biochem.77.083007.093039
- Ratledge, C., and Wynn, J. P. (2002). The biochemistry and molecular biology of lipid accumulation in oleaginous microorganisms. *Adv. Appl. Microbiol.* 51, 1–52. doi: 10.1016/S0065-2164(02)51000-5
- Redfield, A. C. (1958). The biological control of chemical factors in the environment. *Am. Sci.* 46, 205–221.
- Roels, J. A. (1980). Application of macroscopic principles to microbial-metabolism. *Biotechnol. Bioeng.* 22, 2457–2514. doi: 10.1002/bit.260221202
- Rúa, J., de Cima, S., del Valle, P., Gutiérrez-Larraínzar, M., Busto, F., and de Arriaga, D. (2008). Glycogen and trehalose mobilization by acetic acid in *Phycomyces blakesleeanus*: dependence on the anion form. *Res. Microbiol.* 159, 200–206. doi: 10.1016/j.resmic.2008.01.002
- Ruiz, J. A., López, N. I., Fernández, R. O., and Méndez, B. S. (2001). Polyhydroxyalkanoate degradation is associated with nucleotide accumulation and enhances stress resistance and survival of *Pseudomonas oleovorans* in natural water microcosms. *Appl. Environ. Microbiol.* 67, 225–230. doi: 10.1128/AEM.67.1.225-230.2001
- Schimel, J., and Schaeffer, S. M. (2012). Microbial control over carbon cycling in soil. *Front. Microbiol.* 3:348. doi: 10.3389/fmicb.2012.00348
- Schimel, J. P., and Weintraub, M. N. (2003). The implications of exoenzyme activity on microbial carbon and nitrogen limitation in soil: a theoretical model. *Soil Biol. Biochem.* 35, 549–563. doi: 10.1016/S0038-0717(03)00015-4
- Schleuss, P.-M., Widdig, M., Heintz-Buschart, A., Guhr, A., Martin, S., Kirkman, K., et al. (2019). Stoichiometric controls of soil carbon and nitrogen cycling after long-term nitrogen and phosphorus addition in a mesic grassland in South Africa. *Soil Biol. Biochem.* 135, 294–303. doi: 10.1016/j.soilbio.2019.05.018
- Sekar, K., Linker, S. M., Nguyen, J., Grünhagen, A., Stocker, R., and Sauer, U. (2020). Bacterial glycogen provides short-term benefits in changing environments. *Appl. Environ. Microbiol.* 86, e00049–20. doi: 10.1128/AEM.00049-20
- Sterner, R. W., and Elser, J. J. (2002). *Ecological Stoichiometry. The Biology of Elements from Molecules to the Biosphere*. Princeton NJ: Princeton University Press. doi: 10.1515/9781400885695
- Tang, J., and Riley, W. J. (2015). Weaker soil carbon-climate feedbacks resulting from microbial and abiotic interactions. *Nat. Clim Change* 5, 56–60. doi: 10.1038/nclimate2438
- Todd-Brown, K. E. O., Hopkins, F. M., Kivlin, S. N., Talbot, J. M., and Allison, S. D. (2012). A framework for representing microbial decomposition in coupled climate models. *Biogeochemistry* 109, 19–33. doi: 10.1007/s10533-011-9635-6
- Tolla, C., Kooijman, S., and Poggiale, J. C. (2007). A kinetic inhibition mechanism for maintenance. *J. Theor. Biol.* 244, 576–587. doi: 10.1016/j.jtbi.2006.09.001
- Turner, C. B., Wade, B. D., Meyer, J. R., Sommerfeld, B. A., and Lenski, R. E. (2017). Evolution of organismal stoichiometry in a long-term experiment with *Escherichia coli*. *R. Soc. Open Sci.* 4:170497. doi: 10.1098/rsos.170497

- Wang, F.-B., and Hsu, S.-B. (2019). A survey of mathematical models with variable quotas. *Taiwan J. Math.* 23, 269–291. doi: 10.11650/tjm/190102
- Watzer, B., and Forchhammer, K. (2018). “Cyanophycin: a nitrogen-rich reserve polymer,” in *Cyanobacteria*, ed. A. Tiwari (London: InTech). doi: 10.5772/intechopen.77049
- Wieder, W. R., Hartman, M. D., Sulman, B. N., Wang, Y.-P., Koven, C. D., and Bonan, G. B. (2018). Carbon cycle confidence and uncertainty: exploring variation among soil biogeochemical models. *Glob. Change Biol.* 24, 1563–1579. doi: 10.1111/gcb.13979
- Wilkinson, J. F. (1963). Carbon and energy storage in bacteria. *J. Gen. Microbiol.* 32, 171–176. doi: 10.1099/00221287-32-2-171
- Wilson, W. A., Roach, P. J., Montero, M., Baroja-Fernández, E., Muñoz, F. J., Eydallin, G., et al. (2010). Regulation of glycogen metabolism in yeast and bacteria. *FEMS Microbiol. Rev.* 34, 952–985. doi: 10.1111/j.1574-6976.2010.00220.x
- Wu, W., Dijkstra, P., and Dippold, M. (2020). ^{13}C analysis of fatty acid fragments by gas chromatography mass spectrometry for metabolic flux analysis. *Geochim. Cosmochim. Acta* 284, 92–106. doi: 10.1016/j.gca.2020.05.032
- Wutzler, T., Zaehle, S., Schrupf, M., Ahrens, B., and Reichstein, M. (2017). Adaptation of microbial resource allocation affects modelled long term soil organic matter and nutrient cycling. *Soil Biol. Biochem.* 115, 322–336. doi: 10.1016/j.soilbio.2017.08.031
- Xu, X., Thornton, P. E., and Post, W. M. (2013). A global analysis of soil microbial biomass carbon, nitrogen and phosphorus in terrestrial ecosystems. *Glob. Ecol. Biogeogr.* 22, 737–749. doi: 10.1111/geb.12029
- Conflict of Interest:** The authors declare that the research was conducted in the absence of any commercial or financial relationships that could be construed as a potential conflict of interest.
- Publisher’s Note:** All claims expressed in this article are solely those of the authors and do not necessarily represent those of their affiliated organizations, or those of the publisher, the editors and the reviewers. Any product that may be evaluated in this article, or claim that may be made by its manufacturer, is not guaranteed or endorsed by the publisher.
- Copyright © 2021 Manzoni, Ding, Warren, Banfield, Dippold and Mason-Jones. This is an open-access article distributed under the terms of the Creative Commons Attribution License (CC BY). The use, distribution or reproduction in other forums is permitted, provided the original author(s) and the copyright owner(s) are credited and that the original publication in this journal is cited, in accordance with accepted academic practice. No use, distribution or reproduction is permitted which does not comply with these terms.